Data Availability Statement

Our Mandates Data Policy requires data to be shared and a Data Availability Statement, so please enter one in the space below. Sample statements can be found here. Please note that this statement will be published alongside your manuscript, if it is accepted for publication.

The data that support the findings of this study are available from the corresponding author upon reasonable request.

CHUP1 restricts chloroplast movement and effector-triggered immunity in epidermal cells

Alexander O. Nedo[1,2,3], Huining Liang[4], Jaya Sriram[1,2], Md Abdur Razzak[1,2], Jung-Youn Lee[1,2,3], Chandra Kambhamettu[4], Savithramma P. Dinesh-Kumar[5*], and Jeffrey L. Caplan[1,2,3*]

[1]Department of Plant and Soil Sciences, University of Delaware, Newark, DE, 19716 USA
[2]Delaware Biotechnology Institute, University of Delaware, Newark, DE, 19713 USA
[3]Department of Biological Sciences, University of Delaware, Newark, DE, 19716 USA
[4]Department of Computer & Information Sciences, University of Delaware, Newark, DE, 19716 USA
[5]Department of Plant Biology and The Genome Center, College of Biological Sciences, University of California, Davis, CA, 95616 USA

*Co-corresponding authors: jcaplan@udel.edu; spdineshkumar@ucdavis.edu

ORCID

Alexander O. Nedo 0000-0002-0824-315X
Huining Liang 0009-0000-9781-2651
Md Abdur Razzak 0000-0002-2576-8142
Jung-Youn Lee 0000-0003-4604-7974
Chandra Kambhamettu 0000-0001-5306-3994
Savithramma P. Dinesh-Kumar 0000-0001-5738-316X
Jeffrey L. Caplan 0000-0002-3991-0912

Total word count (excluding summary, references and legends):	7009	No. of Figures:	8 (all in color)
Summary:	192	No. of Tables	0
Introduction:	1282	No. of Embedded Videos	11
Materials and Methods:	958	No. of Supporting Information Files	1 (Fig. S1-S9; Table S1-S4)
Results:	3089		
Discussion:	1680		
Acknowledgements:	28		

Summary

- Chloroplast Unusual Positioning 1 (CHUP1) plays an important role in the chloroplast avoidance and accumulation responses in mesophyll cells. In epidermal cells, prior research showed silencing *CHUP1* induced chloroplast stromules and amplified effector-triggered immunity (ETI); however, the underlying mechanisms remain largely unknown.
- CHUP1 has a dual function in anchoring chloroplasts and recruiting chloroplast-associated actin (cp-actin) filaments for blue light-induced movement. To determine which function is critical for ETI, we developed an approach to quantify chloroplast anchoring and movement in epidermal cells. Our data show that silencing *NbCHUP1* in *Nicotiana benthamiana* plants increased epidermal chloroplast de-anchoring and basal movement, but did not fully disrupt blue-light induced chloroplast movement.
- Silencing *NbCHUP1* auto-activated epidermal chloroplast defense (ECD) responses including stromule formation, perinuclear chloroplast clustering, the epidermal chloroplast response (ECR), and the chloroplast reactive oxygen species (ROS), hydrogen peroxide (H_2O_2). These findings show chloroplast anchoring restricts a multi-faceted ECD response.
- Our results also show that the accumulated chloroplastic H_2O_2 in *NbCHUP1*-silenced plants was not required for the increased basal epidermal chloroplast movement, but was essential for increased stromules and enhanced ETI. This finding indicates that chloroplast de-anchoring and H_2O_2 play separate but essential roles during ETI.

Key words: Chloroplast movement, stromules, effector triggered immunity (ETI), epidermal chloroplast defense (ECD), reactive oxygen species, epidermal chloroplast response (ECR), Chloroplast Unusual Positioning 1 (CHUP1), phototropin 2 (phot2)

Introduction

Plant leaves are complex organs consisting of two mesophyll layers and a vascular system enveloped by an epidermis that typically consists of guard cells, trichomes, and mostly epidermal pavement cells (herein, epidermal cells) (Pyke & López-Juez, 1999). In dicot plant leaves, the main plastids in mesophyll and epidermal cells are chloroplasts and they differ vastly in their size, shape, regulation, and function (Barton *et al.*, 2016). There are more chloroplasts in mesophyll cells that are generally larger with an extensive system of thylakoid stacks, called grana, that contain the photosynthetic light-harvesting machinery (Mustárdy & Garab, 2003; Kunz *et al.*, 2023). These well-developed grana are the site of many light reactions that are essential for mesophyll cells to carry out their primary function, photosynthesis (Andersson & Anderson, 1980; Pyke, 2009). For a long time, it was thought that in most plants, epidermal pavement cells do not have chloroplasts (Pyke, 2009). However, more recent studies show that in the model plants, *Nicotiana benthamiana* and *Arabidopsis thaliana*, there are epidermal chloroplasts that contain chlorophyll, but they are much smaller, with fewer grana, when compared to mesophyll chloroplasts (Barton *et al.*, 2016). There is growing evidence that these epidermal chloroplasts have evolved to become "sensory" organelles with a primary function in receiving and sending signals rather than photosynthesis (Caplan *et al.*, 2008; Trotta *et al.*, 2014; Caplan *et al.*, 2015; Barton *et al.*, 2016; Beltran *et al.*, 2018; Dopp *et al.*, 2021; Irieda & Takano, 2021).

Chloroplasts can sense changes in the environment, including biotic stresses like pathogen ingress. To this end, chloroplasts act as primary producers of defense-related compounds, like reactive oxygen species (ROS), such as hydrogen peroxide (H_2O_2), and salicylic acid (SA) (Yang *et al.*, 2021). The generation of ROS has been implicated in different types of innate immune responses, however, with some key differences between them. A rapid singular burst of ROS occurs during pattern-triggered immunity (PTI) in response to recognition of pathogen-associated molecular patterns (PAMPs) by cell surface localized pattern recognition receptors (PRRs) (Yu *et al.*, 2017). In comparison, during effector-triggered immunity (ETI) initiated by recognition of pathogen encoded effectors by nucleotide binding leucine rich repeat (NLR) class of immune receptors, there is a first rapid ROS burst and then a second, sustained burst (Torres, 2010). This sustained ROS burst, along with an increase in SA, has been shown to induce a downstream signaling cascade, that often leads to a hypersensitive response, a type of programmed cell death (HR-PCD) (Balint-Kurti, 2019). The sustained ROS burst during ETI is generated through chloroplasts (Liu *et al.*, 2007; Kachroo *et al.*, 2021). We and others have shown that chloroplast-generated ROS can change chloroplast behavior through inducing stroma-filled tubules called stromules,

which play a role in either signal transmission or regulating chloroplast movement (Gray *et al.*, 2012; Brunkard *et al.*, 2015; Caplan *et al.*, 2015; Meier *et al.*, 2023).

Chloroplasts change positioning in response to environmental stimuli, and the vast majority of these studies have been on mesophyll chloroplasts' response to light (Sakai *et al.*, 2001; Kagawa & Wada, 2002; Oikawa *et al.*, 2008; Kadota *et al.*, 2009; Luesse *et al.*, 2010; Whippo *et al.*, 2011; Gotoh *et al.*, 2018). To efficiently collect light for photosynthesis, mesophyll chloroplasts accumulate on the periclinal surface under low light conditions, but will move to the anticlinal walls under high light conditions to avoid photodamage (Kasahara *et al.*, 2002). Mesophyll chloroplast movement has been extensively studied, revealing the role and significance of various major players in this accumulation and avoidance response. Photoreceptors phototropin 1 (phot1) and 2 (phot2) trigger these light-based responses (Jarillo *et al.*, 2001; Kagawa *et al.*, 2001; Sakai *et al.*, 2001), as well as light-based responses in other tissue types, such as stomatal opening and closing and leaf expansion during plant growth (Kinoshita *et al.*, 2001; Takemiya *et al.*, 2005). Epidermal chloroplasts also respond to blue light, and the studies on epidermal chloroplast positioning have focused on their role in nuclear avoidance movement (Higa *et al.*, 2014; Suetsugu *et al.*, 2015; Suetsugu *et al.*, 2016).

During ETI, epidermal chloroplasts send out stromules that connect to nuclei, and this leads to perinuclear clustering of chloroplasts, potentially increasing the transmission of chloroplast-generated defense signals, as we were able to observe movement of chloroplastic N-receptor interacting protein 1 (NRIP1) being transported into the nucleus from the chloroplasts (Caplan *et al.*, 2015). Formation of stromules is dependent on calponin homology domain containing kinesin (KIS1), with its microtubule-binding motor domain being required for stromule formation while its Calponin homology domain is required for actin binding and perinuclear clustering of chloroplasts (Meier *et al.*, 2023). Perinuclear clustering is not specific to ETI, but occurs under other environmental stress and has been implicated more generally in retrograde signaling and inter-organelle communication (de Souza *et al.*, 2017; Ding *et al.*, 2019). Epidermal chloroplasts have also been shown to reposition in response to infection by fungi and oomycetes. During *Phytophthora infestans* infection, chloroplasts with stromules accumulate around haustoria (Savage *et al.*, 2021). Upon infection by non-adapted fungi, Arabidopsis plants initiate a non-host response (NHR) that invokes an epidermal chloroplast response (ECR) during which chloroplast reposition to the surface of the cell (Irieda & Takano, 2021). Collectively, the emerging

evidence points to chloroplast likely having a robust sensing and signaling role in epidermal cells across a wide range of responses.

A major breakthrough in understanding mechanistic basis of mesophyll chloroplasts repositioning was the discovery of Chloroplast Unusual Positioning 1 (CHUP1), which is required for blue light-based accumulation and avoidance responses (Oikawa *et al.*, 2003; Oikawa *et al.*, 2008; Kong *et al.*, 2013). These studies also show that CHUP1 plays a role in mesophyll chloroplast anchoring because in *chup1* mutants there is an increase in the aggregation of chloroplasts. The *chup1* mutant was found in a genetic screen by examining light transmission through leaves, which changes during the accumulation and avoidance responses. That general screening approach was fruitful, and discovered other key players in chloroplast positioning, including KINESIN-LIKE PROTEIN FOR ACTIN-BASED CHLOROPLAST MOVEMENT 1 (KAC1) and 2 (KAC2) (Suetsugu *et al.*, 2010), PLASTID MOVEMENT IMPAIRED1 (PMI1) and 2 (PMI2) (DeBlasio *et al.*, 2005), J-domain protein required for chloroplast accumulation response 1 (JAC1) (Suetsugu *et al.*, 2005), and THRUMIN 1 (Whippo *et al.*, 2011). Beyond improper blue light-based accumulation and avoidance, these mutants have other similarities, such as a general increase in the aggregation of chloroplasts in *chup1* and *kac1 mutants*, indicating that they play a significant role in chloroplast anchoring (Oikawa *et al.*, 2008; Suetsugu *et al.*, 2010). Mechanistic studies discovered that CHUP1 generates the motive force by playing a critical role in the recruitment of actin to the leading edge of chloroplasts outer membrane (cp-actin) in mesophyll cells (Kadota *et al.*, 2009; Kong *et al.*, 2024) and in epidermal cells for nuclear movement (Higa *et al.*, 2014; Suetsugu *et al.*, 2016). This recruitment of cp-actin and organization of actin microfilaments has been further associated with other movement related players, such as THRUMIN1, implying that CHUP1 is a critical part of a larger complex, driving chloroplast movement as an actin polymerization factor in mesophyll cells (Dwyer & Hangarter, 2021; Kong *et al.*, 2024).

Much less is known about the role of CHUP1 in epidermal cells during plant innate immunity. Here, we show that in epidermal cells, CHUP1's main role is in chloroplast anchoring because silencing of *CHUP1* increases rather than decreases chloroplast movement and repositioning. This increase in chloroplast movement is independent of phot*2* photoreceptor and cp-actin, indicating that a novel mechanism(s) is involved in epidermal chloroplast movement compared to mesophyll chloroplasts. Our findings described here further show that *CHUP1*-mediated anchoring is important for proper regulation of epidermal chloroplast movement and epidermal chloroplast defense (ECD) during immunity.

Materials and Methods

Agrobacterium-based transient expression

Agrobacterium tumefaciens transient expression was conducted as described in (Caplan *et al.*, 2015; Kumar *et al.*, 2018). Constructs were transformed into Agrobacterium strains GV2260 or GV3101 and grown on LB plates with antibiotic selection (Supplemental Table S1). *Agrobacterium* was suspended in infiltration media containing 10 mM $MgCl_2$, 10 mM 2-Morpholinoethanesulfonic acid (MES) and 200 µM acetosyringone and diluted to a final OD_{600} of 0.5. The *Agrobacterium* was incubated for a minimum of 3 hours prior to infiltration into the 5th or 6th leaves of *Nicotiana benthamiana* using a 1 mL needleless syringe. See Supporting Information (Methods S1) for plant growth conditions. Plants were left at room temperature for 16-24 hours under ambient light conditions before being placed back into the growth chamber. Standard agroinfiltration expression of fluorescent protein fusions were imaged 48- or 72-hours post infiltration (Table S1).

Virus-induced gene silencing

N. benthamiana transgenic plants expressing the N NLR immune receptor were used for *Tobacco rattle virus* (TRV)- based virus-induced gene silencing (VIGS) experiments as described in (Liu *et al.*, 2002; Dinesh-Kumar *et al.*, 2003). Agrobacterium containing TRV1 was mixed with cultures containing TRV2 empty vector, TRV2:*NbCHUP1*, TRV2:*Nbphot2*, TRV2:*NbCHUP1Nbphot2*, TRV2:*Nbphot1*, and TRV2:*NbCHUP1Nbphot1* in a 1:1 ratio adjusting the final OD_{600} to 0.5 in infiltration media. Three week-old plants were infiltrated and imaged 13 days post infiltration. VIGS efficiency was measured by quantitative real-time PCR (Supporting Information Methods S2 and Table S2).

Imaging of chloroplast and stromule dynamics

Images for stromule and chloroplast movement dynamics were collected using super-resolution fast Airyscan on a Zeiss LSM880 laser scanning confocal microscope with a C-Apochromat 40X water immersion objective lens [numerical aperture (NA)=1.2]. In the low and high intensity blue light experiments, the same leaf sample was first imaged with only low intensity (3.70 µW) 514 nm green laser, and then after 9 minutes, the leaf sample was exposed to additional high intensity (24 µW) 458 nm blue light laser for an additional 9 minutes. For *Arabidopsis thaliana* experiments, the duration of images was cut in half to 4 minutes and 30 seconds and for examining the effects of red light the blue light laser was exchanged for a red-light laser, all other conditions were kept the same (See Table S3 for

power levels). In experiments inducing ETI, different leaf slices were imaged individually without any blue light laser present. Airyscan images were processed using Zen Black version 3.0 (Carl Zeiss). Maximum intensity projections (MIPs) were created using Fiji, a version of ImageJ (Schindelin *et al.*, 2012). Fiji was used to correct instances of field of view drift in processed Airyscan images using the plugin "Linear Stack Alignment with SIFT'' (Lowe, 2004). Lifeact-TagRFP (actin), mTalin-GFP (actin) (Dyachok *et al.*, 2014), and RBCS1a$_{cTP}$-mNG (chloroplasts and stromules) were imaged under high intensity blue light on an Andor Dragonfly 600. Borealis total internal reflection fluorescence (BTIRF) microscopy was conducted with a HC PlanApochromat 63x TIRF oil immersion lens (NA 1.47) cTP-mNG was imaged using a 488nm laser and Lifeact-TagRFP was imaged with a 561 nm laser. Spinning disk confocal microscopy was conducted using a Leica HC Plan Apochromat CS2 40X water immersion objective lens (NA 1.1). Datasets which experienced uncorrectable image drift or showed cellular damage or death caused by infiltration were discarded. See Supporting Information for detailed methods of image analysis (Methods S3), a description of metrics (Table S4), and the analyzed datasets (Table S5).

Confocal Imaging of cytoplasmic streaming

Cytosolic streaming was visualized in *N. benthamiana* using transient expression of p35S::Citrine and in *A thaliana* using 2 µM concentrations of 5-Chloromethylfluorescein diacetate (Green CMFDA). CMFDA was then infiltrated into a leaf and mounted in a NUNC chamber for 10-15 minutes prior to imaging. Cytochalasin D treatments were performed as previously described (Kumar et al., 2018; Methods S4). Spinning disk images were deconvolved, drift corrected, and bleach corrected using Huygens software (Scientific Volume Imaging).

Measurement of H_2O_2 with HyPer7 sensor

HyPer7 ratiometric measurements of H_2O_2 were collected on a Andor Dragonfly 600 spinning disk confocal microscope (Oxford Instruments) using a Leica HC Plan Apochromat CS2 40X water immersion objective lens (NA 1.1). Excitation laser powers with the 405 nm and 488 nm lasers were optimized to induce no additional ROS during imaging (Supplemental Table S3). Ratiometric measurements of fluorescence emission (521/38nm bandpass filter) using 488 nm excitation and 405 nm excitation were calculated in FIJI. Ratiometric images using a "fire" lookup table in FIJI were created for visual display.

Statistical analysis

Statistical analysis was performed using Prism 7 or 9 (Graphpad). For normally distributed data such stromule induction, frequency of chloroplast movement, # of chloroplast per nucleus, ECR, and frequency of SDM and Chl-Chl movement, Student's t-test with Welch's correction was performed when comparing two groups, while a Welch's analysis of variance (ANOVA) with Dunnett's T3 multiple comparison test was performed when comparing multiple groups. For non-normally distributed data such as maximum stromule length, maximum change in stromule length, stromule tip velocity, chloroplast body velocity, snake curvature, snake length and HyPer7 ratio were calculated using a Mann-Whitney U-test for comparing two groups and a Kruskal-Wallis with Dunn's multiple comparisons test for comparing data sets with more than two groups. Different letters signify significant difference and groups with and without the prime symbol (') were compared separately. For all data containing HyPer7 ratios, a minimum of three biological plant replicates were used for each condition. For all other data, there were a minimum of eight biological plant replicates unless otherwise stated. All data is comprised from at least three experimental replicates unless otherwise stated. In data represented as percentages or ratios the N values are the number of leaf sections. For Hyper7, chloroplast velocity, stromule tip velocity, and stromule length graphs the N values are individual chloroplasts or stromules.

Results

CHUP1-silencing promotes increased chloroplast movement in epidermal pavement cells

In a prior study, we discovered that knockdown of *CHUP1* expression using TRV-based VIGS in *N. benthamiana* and knockout of *CHUP1* in Arabidopsis resulted in an increase in the amount of chloroplast stromules in epidermal cells and enhanced HR-PCD during ETI (Caplan *et al.*, 2015). Since CHUP1 is required for chloroplast movement in mesophyll cells (Oikawa *et al.*, 2003), we posited that the increase in stromules may be caused by a change in chloroplast movement. To study this, we silenced *CHUP1* (Fig. S1) and quantified basal chloroplast movement, chloroplast movement that is not induced by light. For all experiments, we used upper leaves that had more efficient silencing (Fig. S1), similar TRV transcript levels as the VIGS control (Fig. S2a), and no TRV symptoms (Fig. S2c). Silencing *CHUP1* nearly tripled the percentage of chloroplasts moving and increased their velocity in epidermal cells (Fig. 1a-b). To examine this further, we quantified the number of chloroplasts that had connected chloroplast-to-chloroplast (Chl-Chl) movement. When chloroplast anchoring is disrupted, chloroplasts will aggregate and two or more chloroplasts will associate with each other and move together (Oikawa *et al.*, 2008; Yang *et al.*, 2011; Suetsugu *et al.*, 2012; Savage *et al.*, 2021). Connected Chl-Chl movement was greatly increased in epidermal cells of *CHUP1*-silenced plants compared to the control (Fig. 1c).

241

242 Alternatively, CHUP1 may only be required for chloroplast movement in epidermal cells in response to
243 high intensity light similar to chloroplast avoidance response in mesophyll cells. Therefore, we
244 quantitated chloroplast movement and velocity in epidermal cells under low intensity light (LL) and high
245 intensity blue light (HL) in wild-type and *CHUP1*-silenced plants. In the control plants, the percentage of
246 moving epidermal chloroplasts and their velocity increased in response to HL (Fig. 1d-e; Video 1, Video
247 2). However, in *CHUP1*-silenced plants, the percentage of moving epidermal chloroplasts was higher
248 with or without HL, which was similar to control plants with HL (Fig. 1d-e; Video 1, Video 3). In terms of
249 velocity, there was additional increase in response to HL compared to LL (Fig. 1f). Next, to determine if
250 Arabidopsis *chup1* mutants exhibit similar phenotypes, we performed these experiments in *Atchup1*
251 plants. Similar to *CHUP1*-silenced *N. benthamiana* plants, we found increased basal epidermal
252 chloroplast movement under LL conditions in *Atchup1* compared to wild-type Col-0 plants (Fig. 1g).
253 Furthermore, we found an increase in the percent of chloroplasts moving and chloroplast velocity under
254 HL when compared to LL in *Atchup1* (Fig. 1g-h). In comparison, silencing *CHUP1* in *N. benthamiana* did
255 not increase in the percent of chloroplasts moving and a lower increase in chloroplast velocity (Fig. 1e-f).
256

257 To determine if this was a blue light-induced response and not simply due to an increase in
258 photosynthetic activity, we repeated the experiments using high red light. High red light did not further
259 increase chloroplast movement or velocity in the *NbCHUP1*-silenced or *Atchup1* plants (Fig. S3). We
260 observed a slight decrease in velocity in Col-0 when exposed to high intensity red light, but no
261 statistically significant change in *Atchup1* mutant (Fig. S3b). These results suggest that there is a CHUP1
262 independent pathway for blue light-induced chloroplast movement in epidermal cells.
263

264 In mesophyll cells, the chloroplast avoidance response requires blue light photoreceptor, phot2, and to
265 lesser extent phot1 (Jarillo *et al.*, 2001; Kagawa *et al.*, 2001; Sakai *et al.*, 2001; Luesse *et al.*, 2010).
266 Therefore, we silenced *PHOT1* and *PHOT2 in N. benthamiana* (Fig. S1) and then examined basal and
267 light-induced epidermal chloroplast movement. Silencing *PHOT2* disrupted the HL-induced increased in
268 epidermal chloroplast movement and velocity (Fig. 1d-f; Video 1, Video 4). Silencing *PHOT1* had no
269 effect on HL-induced chloroplast movement (Fig. 1d-e), but increased HL-induced epidermal chloroplast
270 velocity (Fig. 1f). These data are in agreement with studies in Arabidopsis *phot1* mutants that have a
271 faster mesophyll chloroplast avoidance response (Ichikawa *et al.*, 2011), and indicate that similar to
272 mesophyll cells, HL-induced epidermal chloroplast movement primarily requires phot2.

Next, we tested if this constitutive movement in *CHUP1*-silenced plants is dependent on phot2. Co-silencing *CHUP1* with *PHOT2* or *PHOT1* did not disrupt the increased chloroplast movement and chloroplast velocity caused by *CHUP1*-silencing (Fig. 1d-f; Fig. S1; Video 1, Video 4), indicating that the *CHUP1*-silencing effect is dominant and overrode the disruption of chloroplast movement by *PHOT2* silencing. Together, these results indicate that CHUP1 is not required for increased epidermal chloroplast movement in response to HL, and rather, more likely functions during chloroplast anchoring.

Cytoplasmic streaming partially contributes to chloroplast movement in an actin dependent manner

In mesophyll cells, light-induced chloroplast movement has been shown to be dependent on actin microfilaments, with accumulation of cp-actin filaments playing a critical role in the blue light avoidance response (Kadota *et al.*, 2009; Suetsugu *et al.*, 2016; Wada & Kong, 2018; Dwyer & Hangarter, 2021; Dwyer & Hangarter, 2022). We were unable to observe cp-actin filaments on epidermal chloroplasts showing phototrophic movement in response to HL using total internal reflection fluorescence microscopy (Fig. S4a) or spinning disk confocal microscopy (Fig. 2a-b, Fig. S4b-d; Note S1; Video 5, Video 6, Video 7), suggesting alternative modes of chloroplast movement. Since we were unable to observe cp-actin in epidermal cells, we next examined the role of cytoplasmic streaming during basal and blue light induced chloroplast movement. For these experiments, we marked the cytoplasm by transiently expressing free Citrine in *N. benthamiana* or using a green tracer dye, CMFDA, in *A. thaliana*. First, we examined blue light movement in wild-type *N. benthamiana* and Arabidopsis plants. We identified instances in which chloroplasts were stationary and anchored under low light, but rapidly moved with a cytoplasmic stream under high light (Fig. 3a, Video 8). We categorized chloroplast movement that directly correlates with cytoplasmic streams as a form of rapid linear movement. Next, we examined the effect of *CHUP1* silencing. In the VIGS control, we again observed chloroplasts moving with cytoplasmic streaming under high light conditions (Fig. S5a, Video 9). In the *CHUP1*-silenced plants, we observed partial correlation of chloroplast movement with cytoplasmic streaming with low or high light conditions. For example, we observed an instance of a chloroplast first moving within a cytoplasmic stream before moving away from the stream and eventually released, moving independently from cytoplasmic streaming (Fig. 3b; Fig. S5a, Video 9). These data suggest that when chloroplasts are de-anchored, increased chloroplast movement is partially correlated with movement in cytoplasmic streaming.

Next, we disrupted cytoplasmic streaming using an actin polymerization inhibitor, cytochalasin D (CD), and examined chloroplast movement. Cytochalasins have been used previously to disrupt and study cytoplasmic streaming (Foissner & Wasteneys, 2007; Poulsen *et al.*, 2013; Holzinger & Blaas, 2016). CD completely abolished cytoplasmic streaming in *N. benthamiana* (Fig. 3c, Video 9) and Arabidopsis plants (Video 10). CD also inhibited chloroplast movement as we observed previously (Kumar *et al.*, 2018). Quantification showed that CD reduced basal chloroplast movement and eliminated light-induced chloroplast movement in both *N. benthamiana* (Fig. 3d, Video 9) and Arabidopsis (Fig. 3e, Video 10). Furthermore, CD disrupted the increase of basal chloroplast movement in *CHUP1*-silenced (Fig. 3d) and *Atchup1* plants (Fig. 3e). To quantify chloroplast movement that was heavily correlated and potentially driven by cytoplasmic streaming, we counted the proportion of chloroplasts which exhibited rapid linear movement in cytoplasmic streams (see representative examples in Fig. 3a and Fig. S5). CD completely abolished this type of chloroplast movement in *CHUP1*-silenced and *Atchup1* plants (Fig. S6), but did not abolish all chloroplast movement (Fig. 3d,e). These findings suggest chloroplast anchoring prevents chloroplasts from moving in cytoplasmic streams and de-anchoring chloroplasts with high blue light or disrupting CHUP1 function allows chloroplasts to partially move with cytoplasmic streaming in epidermal cells.

CHUP1-silencing increases chloroplast stromule dynamicity

Next, we performed a more detailed examination of stromules to determine if they play a role in the constitutive increase in chloroplast movement caused by either *CHUP1* silencing or HL. First, we confirmed that *CHUP1* silencing induces stromules (Fig. 4a-b) as we and others have previously reported (Caplan *et al.*, 2015; Irieda & Takano, 2021). We then examined if epidermal chloroplasts follow the direction of stromules, which is a type of movement previously described as stromules directed movement (SDM) of chloroplasts (Fig. S7). In *CHUP1*-silenced plants, there was no increase in the percentage of stromule movement events causing SDM (Fig. 4c). Since there was an overall increase in chloroplast movement, SDM represented a lower percentage of total chloroplast movement (Fig. 4d). These data indicate that the observed increased chloroplast movement in *CHUP1*-silenced plants was not due to SDM.

Next, a custom stromule tracking program in MATLAB was developed and used to quantify various stromule movement characteristics under LL and HL in various silenced plants (Fig. S7b-c). We observed increased stromule velocity, length, and max length change in *CHUP1*-silenced plants (Fig. 4e-g) and there was no further change in response to HL (Fig. S8b-c). There was no change in the amount of

stromule extensions or retractions in *CHUP1*-silenced plants compared to the control silenced plants (Fig. S9). Furthermore, the stromule quantity, tip velocity, and length did not change in response to HL in the silencing control plants and in *PHOT2*-silenced plants (Fig. S8a-c). Interestingly, silencing *PHOT1* increased stromule tip velocity in response to HL (Fig. S8b) and constitutively increased the length of stromules even in LL (Fig. S8c). In *CHUP1PHOT1*-silenced plants there was a further increase in stromule tip velocity in response to HL (Fig. S8b), but there was no further increase in stromule length (Fig. S8c). Therefore, it is possible that phot1 inhibits stromule movement in response to HL via the same mechanism that it inhibits chloroplast movement in mesophyll chloroplasts (Ichikawa *et al.*, 2011). Together, our results indicate that stromule movement, like chloroplast movement, is more dynamic in *CHUP1*-silenced plants, suggesting chloroplast anchoring may inhibit stromules dynamicity.

CHUP1-silencing amplifies immunity associated chloroplast responses

It is now well established that chloroplasts are an integral part of the plant innate immune system, playing multifaceted roles during the defense against pathogens (Kumar *et al.*, 2018; Park *et al.*, 2018; Kachroo *et al.*, 2021; Irieda, 2022). We previously showed that silencing *CHUP1* or knocking out *Atchup1* amplifies the hypersensitive response type of PCD during ETI (Caplan *et al.*, 2015), and, the data presented above suggests that *CHUP1* silencing disrupts chloroplast anchoring. Therefore, we examined three key components of the epidermal chloroplasts defense (ECD) in *CHUP1*-silenced plants. *CHUP1* silencing constitutively induced stromules to a level similar to stromule induction during ETI in control plants (Fig. 5a). In *CHUP1*-silenced plants there was no further increase in stromules during ETI (Fig. 5a). Similarly, in *CHUP1*-silenced plants, there was a constitutive increase in stromule tip velocity, maximum length, and maximum length change, and no further significant increase during ETI (Fig. 5b-d). Silencing *PHOT2* had a no effect on stromule dynamics during ETI (Fig. S10a-c), but silencing *PHOT1* disrupted any increased stromule velocity during ETI, which was restored by co-silencing with *CHUP1* (Fig. S10a-b). Taken together with the increase in stromule length and tip velocity in *PHOT1*-silenced plants observed in the light intensity experiments (Fig. S8b-c), it is possible that *phot1* may negatively regulate stromules by an unknown mechanism.

Next we examined perinuclear chloroplast clustering. During ETI, epidermal chloroplasts move towards nuclei, resulting in perinuclear clustering (Kumar *et al.*, 2018; Meier *et al.*, 2023). Furthermore, *CHUP1* has been implicated in chloroplast-driven nuclear movement and an increase in perinuclear clustering in *Atchup1* mutant has been reported (Higa *et al.*, 2014; Suetsugu *et al.*, 2016). In *CHUP1*-silenced plants,

perinuclear chloroplast clustering was constitutively induced (Fig. 5e-f). The level of clustering in *CHUP1*-silenced plants was higher than the level induced during ETI in the control silenced plants (Fig. 5f). Furthermore, we found that expression of *CHUP1* RNA is increased rather than decreased during ETI (Fig. S11), suggesting that the *CHUP1* controlled de-anchoring occurs post-transcriptionally.

Lastly, we examined the ECR, which was first described as a non-host response during fungal infection and was shown to be increased in *Atchup1* mutant (Irieda & Takano, 2021). ECR has not been studied during ETI, and here, we show that ECR is also induced during ETI (Fig. 6a-b). Silencing *CHUP1* constitutively increased ECR similar to the level induced during ETI (Fig. 6a-b). ECR was further increased during ETI in *CHUP1*-silenced plants (Fig. 6a-b). Together, all three of the ECD responses examined were constitutively activated in *CHUP1*-silenced epidermal cells, and then further amplified during ETI. The ECD responses are not simply a result of increased random epidermal chloroplast movement, since the percentage of moving chloroplasts did not increase during ETI and there is just a minor increase in chloroplast velocity (Fig. 6c-d, Fig. S10d-e). Our findings indicate that the general, constitutive amplification of ECD may lead to a priming of ETI, explaining the previously reported increased rate of ETI-induced cell death in *CHUP1*-silenced or *Atchup1* knockout plants (Caplan *et al.*, 2015).

CHUP1-silencing increases epidermal chloroplastic ROS that is responsible for stromule induction and enhanced cell death during ETI

The results described above established that ECD responses related to chloroplast positioning and stromule movement are increased in *CHUP1*-silenced epidermal cells. To explore if defense signals are also elevated in *CHUP1*-silenced epidermal chloroplasts, we focused on H_2O_2 because of its well-established role as a ROS signal during ETI (Shapiguzov *et al.*, 2012; Caplan *et al.*, 2015; Jwa & Hwang, 2017). To quantitate chloroplastic H_2O_2, we targeted the genetically-encoded H_2O_2 biosensor, HyPer7 (Pak *et al.*, 2020), to the chloroplast stroma by fusing it to Arabidopsis Ribulose Bisphosphate Carboxylase Small Chain 1a (RBCS1a) transit peptide (cTP-HyPer7). As previously reported using the original HyPer sensor (Caplan *et al.*, 2015), cTP-HyPer7 detected an increase in H_2O_2 during ETI, as indicated by the increased ratio of 488 nm to 405 nm excited fluorescence (Fig. 7a-b). In *CHUP1*-silenced epidermal cells, chloroplastic H_2O_2 levels were slightly elevated, but did not increase during ETI to the same level observed in the silencing control plants (Fig. 7b). To determine if this increase in H_2O_2 requires light, we dark adapted the plants 20-22 hours prior to imaging. H_2O_2 levels were lower in the dark adapted *CHUP1*-silenced and silencing control plants compared to plants kept under light (Fig. S12).

Furthermore, we no longer observed the increased level of H_2O_2 in *CHUP1*-silenced plants, suggesting it is light dependent. To determine if other disruptions in light regulated chloroplast positioning elevated H_2O_2, we examined H_2O_2 in *PHOT2* and *PHOT2CHUP1*-silenced plants and found similar light-dependent increases in H_2O_2 (Fig. S12).

Next, to determine if the elevated levels of H_2O_2 contributed to the enhanced PCD during ETI observed in *CHUP1*-silenced plants, we scavenged chloroplastic H_2O_2 by expressing cytosolic ascorbate peroxidase (APX) in the chloroplast stroma. This approach has been used extensively to decrease chloroplastic H_2O_2 by overexpressing native stromal, thylakoid, or cytosolic APX targeted to chloroplasts (Yabuta *et al.*, 2002; Badawi *et al.*, 2004; Exposito-Rodriguez *et al.*, 2017; Dopp *et al.*, 2023). Here, a RBCS1a chloroplast transit peptide was placed on the N-terminus of a cytosolic Arabidopsis APX1 and the fluorescent protein mKate2 was placed on the C-terminus to mark epidermal chloroplasts transiently expressing APX (herein cTP-APX; Fig. S13). Epidermal chloroplasts expressing cTP-APX had a lower level of H_2O_2 prior to ETI and the increase of H_2O_2 was mostly, but not completely, quenched during ETI (Fig. 7c). To examine the effect of silencing *CHUP1* and cTP-APX on PCD, we induced ETI and quantitated it via an ion leakage assay (Hatsugai & Katagiri, 2018). *CHUP1*-silenced plants had elevated levels of ion leakage prior to ETI and an enhanced amount of ion leakage during ETI compared to the silencing control (Fig. 7d; Methods S5). The ion leakage assay showed that overexpression of chloroplast-targeted APX reduced PCD during ETI, and in *CHUP1*-silenced plants, the PCD during ETI was lowered to a level similar to silencing control without APX (Fig. 7d-e). These results indicate that silencing of *CHUP1* increases epidermal chloroplastic ROS production during ETI and this in turn is required for stromule induction and enhanced PCD during ETI.

Epidermal chloroplast movement is independent of chloroplastic ROS

To determine if chloroplastic H_2O_2 is required for other changes in *CHUP1*-silenced plants, we examined the effect of overexpressing chloroplast targeted APX on two key phenotypes, increased chloroplast movement and stromules. Overexpression of cTP-APX did not disrupt the increased chloroplast movement phenotype of silencing *CHUP1* (Fig. S14), suggesting elevated H_2O_2 levels are not required to disrupt anchoring. However, expression of cTP-APX resulted in a partial decrease in stromule induction in *CHUP1*-silenced plants, but had little effect on the stromule induction in the silencing control (Fig. 8a). To further explore the role of H_2O_2 during ETI, we used HL to induce H_2O_2, which has been used previously with HyPer7 to examine redox dynamics and ROS scavenging in epidermal chloroplasts (Dopp

et al., 2023). Plants expressing HyPer7 were exposed to HL and changes in H_2O_2 were measured over 10 minutes (Fig. 8b; Fig. S15; Video 11). This experimental approach made it possible to examine the maximum H_2O_2 scavenging ability in the chloroplast stroma and to further examine the interplay between ETI-induced and HL-induced changes in epidermal chloroplast dynamics. In the silencing control plants, H_2O_2 levels during ETI were higher at the beginning (T=0) and rapidly peaked to very high levels (T=~1.5 min) with HL (Fig. 8b, yellow arrow). The same rapid increase was observed in *CHUP1*-silenced plants during ETI, but it did not peak at the same level as the silencing control during ETI (Fig. 7b, purple arrow). We hypothesize that the constitutive induction of H_2O_2 by silencing *CHUP1* may cause chloroplasts to compensate by increasing their H_2O_2 scavenging capacity. Even without ETI in *CHUP1*-silenced plants, H_2O_2 levels were higher at the beginning of light induction and peaked around the same level (Fig. 8b). To verify that H_2O_2 scavenging affects H_2O_2 levels, we overexpressed cTP-APX and found that the H_2O_2 levels remained relatively low, and had similar response curves to light induction, but at a much lower level (Fig. 8b). The intensity of light we used for this experiment was comparable to the light-induced chloroplast movement experiments shown in Fig. 1. Therefore, we tested the effect of chloroplast-targeted APX on chloroplast movement and stromules under LL and HL. Chloroplast-targeted APX did not disrupt the increased chloroplast movement in *CHUP1*-silenced plants (Fig. 8c). Stromules are not induced by HL, but scavenging H_2O_2 with cTP-APX partially disrupts stromule induction in *CHUP1*-silenced plants with or without HL (Fig. 8d). These results firmly establish that the stromule induction caused by silencing *CHUP1* is at least partially due to an increase in chloroplastic H_2O_2, but the increased chloroplast movement caused by silencing *CHUP1* or HL in epidermal cells is independent of chloroplastic H_2O_2.

Discussion

Our data shows that silencing *CHUP1* leads to an increase in basal chloroplast movement in epidermal cells and points to a differential function of *CHUP1* in epidermal and mesophyll cells. Prior studies examined the epidermal chloroplast avoidance response indirectly through the movement of nuclei (Higa *et al.*, 2014; Suetsugu *et al.*, 2015; Suetsugu *et al.*, 2016). Here, we directly show that epidermal chloroplasts, despite not being used primarily for energy production, do respond to HL and the induced movement is dependent on phot2. This suggests light-regulated chloroplast movement responses are partially conserved between mesophyll and epidermal chloroplasts. However, our study reveals a major difference during ETI. CHUP1 or cp-actin is not required for basal chloroplast movement or chloroplast repositioning during ETI, suggesting CHUP1's primary function in epidermal cells during ETI is in

chloroplast anchoring rather than providing the motive force for chloroplast movement and repositioning. In light of this major finding, we did a detailed analysis on the effect of disrupting chloroplast anchoring. We mainly took a cell biology approach that leveraged the advantages of live-cell confocal microscopy to quantify how silencing *CHUP1* changes epidermal chloroplast movement, stromules, and chloroplastic ROS during plant innate immunity. Our findings show that silencing *CHUP1* auto-activates ECD responses, including stromule induction, perinuclear chloroplast clustering, ECR, and chloroplastic H_2O_2. Our results from using cTP-APX to scavenge H_2O_2 shows that chloroplastic H_2O_2 is essential for ETI and related stromule induction, but not required for chloroplast movement.

There is an emerging theory that chloroplasts should be divided into two categories: photo-harvesting chloroplasts and sensory chloroplasts. Both types may retain partial functionality of either type, but have become specialized for specific functions. Our study in the widely-used model system, *N. benthamiana*, highlights the need to clearly define which type of chloroplasts are being studied. As we show here, what may be essential for a photo-harvesting chloroplasts in mesophyll cells may not be for sensory chloroplasts in epidermal cells. Our study on epidermal sensory chloroplasts focuses on two of the most critical players for HL-induced movement, CHUP1 and phot2. Our results show that silencing *CHUP1* disrupted the control of anchoring and de-anchoring by phot2. Key to this conclusion was our ability to partially distinguish between epidermal chloroplast anchoring (% moving) and movement (velocity) using advanced time-lapse confocal imaging and chloroplast tracking analysis. The development of this approach opens up the possibility for numerous other future studies on other players in HL-induced movement, such as THRUMIN1, KAC1/2, JAC1, and PMI1/2, and how they function to regulate sensory epidermal chloroplasts (DeBlasio *et al.*, 2005; Suetsugu *et al.*, 2005; Suetsugu *et al.*, 2010; Whippo *et al.*, 2011).

Our study suggests that epidermal chloroplasts may not use cp-actin filaments for basal chloroplast movement, such as stromule-directed movement, or repositioning for ECD responses. Instead, cytoplasmic streaming may play a more prominent role during basal chloroplast movement. Cytoplasmic streaming has been extensively studied in the alga *Chara* and an early study showed that it is disrupted by cytochalasin B (Williamson, 1972; Tominaga & Ito, 2015). We previously showed that the actin inhibitor, CD, completely stops chloroplast movement and also alters chloroplast dynamics (Kumar *et al.*, 2018), but we did not examine cytoplasmic streaming. Here, we directly imaged cytoplasmic streaming by marking the cytosol with a fluorescent protein or tracer dye. We then used fast, time lapse

volumetric imaging which allowed us to examine the relationship of cytoplasmic streaming and chloroplast movement. We observed numerous examples of correlated chloroplast movement and cytoplasmic streaming that were disrupted by CD. However, CD will also stop numerous other biological processes that require actin microfilaments. Targeting myosin XIs might be a more specific way to disrupt cytoplasmic streaming, but it also has been implicated in cytoskeletal modeling, stromule formation, innate immunity, and a multitude of other biological processes (Avisar *et al.*, 2008; Natesan *et al.*, 2009; Sattarzadeh *et al.*, 2009; Cai *et al.*, 2014; Tominaga & Ito, 2015; Wang *et al.*, 2024). As such, examining specific changes in cytoplasmic streaming and how those changes influence basal and blue light-induced chloroplast movement is a promising, but challenging area of future research.

Another intriguing finding from our studies is that an increase in blue light-induced chloroplast movement velocity still occur in *CHUP1*-silenced *N. benthamiana* and *Atchup1* mutant plants, which also showed an increase in the percent of chloroplasts moving. Surprisingly, our silencing experiments suggests this does not require *PHOT1* or *PHOT2*, suggesting an unknown pathway is responsible for HL-induced epidermal chloroplast movement in *CHUP1*-silenced plants. Alternatively, it is possible that the phot1 and phot2 are compensating for each other. Our findings show that silencing *PHOT1* further enhanced chloroplast movement velocity, which agrees with previous reports that phot1 can inhibit phot2-dependent responses and disrupting phot2 allows phot1 to briefly respond to HL in mesophyll cells (Ichikawa *et al.*, 2011; Łabuz *et al.*, 2022). The increase in chloroplast velocity by *PHOT2*-silencing only occurred when co-silenced with *CHUP1,* indicating that chloroplast de-anchoring was required for subsequent increase in chloroplast movement velocity. In the future, it will be interesting to examine the mechanistic basis of chloroplast movement in epidermal cells in the absence of *CHUP1*, including how the light is perceived and the molecular machinery that operates in movement.

Our initial impetus for this study was to determine how stromules are induced in *CHUP1*-silenced plants (Caplan *et al.*, 2015). Since knockout of *Atchup1* prevented chloroplast movement, we posited that a disruption of chloroplast movement by *CHUP1*-silencing allowed stromules to stay extended. However, our data showing an increase in chloroplast movement in *CHUP1*-silenced plants in this study quickly disproved that hypothesis. This led us to do a more in-depth analysis of stromule movement dynamics. We used machine learning to find the stromules and MATLAB program to track the tips of stromules. This analysis revealed that silencing *CHUP1* leads to an increased stromule tip velocity, maximum length, and maximum length change. These findings suggest that stromules are induced in *CHUP1*-silenced

plants because they extend faster, making them longer. The amount of extension and retraction remained unchanged, suggesting that stromule induction was more dependent on changes in velocity and length that stochastically leads to a higher persistence of stromules. Stromules can direct movement (Kumar *et al.*, 2018), but the amount of SDM did not increase in *CHUP1*-silenced plants, suggesting that stromules are not causing the increase in chloroplast movement. Therefore, the kinesin required for inducing stromules 1 (KIS1) (Meier *et al.*, 2023) is unlikely to be required for the chloroplast movement, and instead, an unknown molecular motor is more likely to drive chloroplast movement. That motor is unlikely to be a myosin, since there is no evidence that chloroplasts use myosins for movement (Wada & Kong, 2018). Since both KIS1 and KAC1/2 belong to kinesin family 14, future research into other kinesin-14s will determine if one of them is the unknown motor for chloroplast movement in epidermal cells.

In this study, we coined the term epidermal chloroplast defense (ECD) as a more general term to describe changes in sensory epidermal chloroplasts during immunity. A hallmark of ECD is stromule induction, which precedes another ECD response, perinuclear chloroplast clustering (Caplan *et al.*, 2015). Here we show that silencing *CHUP1* increases these ECD responses and could be the reason for previously observed enhanced PCD during ETI in *CHUP1*-silenced or knockout plants (Caplan *et al.*, 2015). Disruption of *CHUP1* was previously reported to induce ECR, which is the repositioning of epidermal chloroplasts to the cell surface during non-host resistance (NHR) (Irieda & Takano, 2021). The molecular mechanisms for NHR can widely vary, but depending on the plant-pathogen interaction, ETI may be involved (Panstruga & Moscou, 2020). Here, we confirm that silencing *CHUP1* constitutively induces ECR, but also show that ECR more generally occurs during ETI. Both ECR and perinuclear clustering require chloroplast de-anchoring before they can reposition and our data points to *CHUP1* as being involved in the de-anchoring process.

Another ECD response is the induction of H_2O_2 in chloroplasts during PTI and ETI (Liu *et al.*, 2007; Shapiguzov *et al.*, 2012), and like all the other ECD responses we examined, it is increased in *CHUP1*-silenced epidermal chloroplasts. Using APX to quench chloroplastic H_2O_2, we show that it is required for the enhanced PCD in *CHUP1*-silenced plants and partially required for stromule induction. These complement prior studies showing an increase in chloroplastic H_2O_2 during ETI, and that exogenous application of H_2O_2 is sufficient to induce stromules (Brunkard *et al.*, 2015; Caplan *et al.*, 2015). It remains unknown why the loss of *CHUP1* causes an increase in chloroplastic H_2O_2 production. One

possibility is improper chloroplast positioning leads to amplification of H_2O_2 caused by photodamage (Kasahara *et al.*, 2002). This is unlikely, due to the flat shape of epidermal cells and it is unlikely that any type of repositioning could avoid HL, however our data does show that it requires light. Another possibility is that silencing *CHUP1* alters a signaling pathway that induces chloroplastic H_2O_2 or more generally alters the redox state of the cell. Studies show that the H_2O_2 scavenging system in the chloroplasts and cytosol are linked, and disruption of cytosolic APX1 cause a collapse of chloroplastic H_2O_2 scavenging system (Kasahara *et al.*, 2002; Exposito-Rodriguez *et al.*, 2017). The HyPer7 sensor was used previously to examine nonphotochemical quenching (NPQ) H_2O_2 scavenging system in different types of epidermal cells (Dopp *et al.*, 2023). We took a similar approach here and found that chloroplast-targeted APX greatly increased NPQ, preventing both HL-induced and ETI-induced H_2O_2. Interestingly, we found that the response to HL was bimodal, suggesting contributions between two different pools of NPQ scavenging. The contribution of different NPQ pools and the exact reasoning behind the induction of H_2O_2 caused by *CHUP1*-silencing remain unclear and are promising areas of future examination. In general, our study further reinforces the central role of chloroplastic H_2O_2 in stromule induction and PCD during ETI while also illustrating that chloroplast movement is dependent on other signaling mechanisms which allow for proper regulation of chloroplastic H_2O_2 based signaling. Furthermore, our study places CHUP1 and its role in chloroplast anchoring, as a key regulator of ECD and PCD induced during ETI.

Acknowledgements

We thank Dr. John McDonald for his guidance with statistical analysis of the data. We also would like to thank Dr. Elison Blancaflor for the mTalin-GFP construct. This work was funded by the National Institutes of Health R01 grant GM132582 to SPDK, JLC, and CK. This work is also funded partially by the National Science Foundation grant IOS 2054685 to JYL and JLC. Microscopy equipment was acquired with shared instrumentation grants (S10 OD030321 and S10 OD016361) and microscopy access was supported by the NIH-NIGMS (P20 GM103446), the NIGMS (P20 GM139760), and the State of Delaware. This research benefitted from the BioStore data management resource at the University of Delaware Bioinformatics Data Science Core [RRID:SCR_017696] supported by an NIH shared instrumentation grant (NIH S10 OD028725).

Competing interests

The authors declare no competing of financial interests.

Author contributions

AON, SPDK, and JLC conceived the experimental designs. AON and JLC conducted all the microscopy experiments. AON conducted the conductivity assays and JS conducted the RT-PCR. HL, CK, and JLC developed the MATLAB code for stromule analysis. MAR and JYL created and validated the cTP-APX-mKate2 construct. AON, JS, SPDK, and JLC wrote the manuscript with the input from all the authors. JLC and SPDK supervised the project. AON, JS, SPDK, and JLC critically revised the manuscript. SPDK, JLC, CK, and JYL received funding for the project. All authors have reviewed the final version of the manuscript and approved it and therefore are equally responsible for the integrity and accuracy of its content.

Data availability

The analyzed datasets can be found in the Supporting Information Table S5. Raw data that support the findings of this study are available from the corresponding author upon reasonable request.

Figure Legends

Fig. 1. Silencing CHUP1 increases epidermal chloroplast movement. In all the experiments, the chloroplast transit peptide (cTP) of RBCS1a was fused to mNeonGreen (RBCS1a$_{cTP}$-mNG) and transiently expressed in *Nicotiana benthamiana* plants (a-f), or by visualizing chlorophyll autofluorescence in *Arabidopsis thaliana* (g-h). RBCS1a$_{cTP}$-mNG localizes to the stroma, marking both the body of chloroplasts and stromules. (a) Moving epidermal chloroplasts were counted and divided by the total number of chloroplasts per image and displayed as percentages in virus-induced gene silencing (VIGS) vector control (-) and *CHUP1*-silenced plants. N=12 and 10 for respective columns. (b) The epidermal chloroplast body velocities in VIGS vector control (-) and *CHUP1*-silenced plants were tracked and quantitated. N=418 and 276 for respective columns. (c) The number of two or more chloroplasts connected and moving together (Chl-Chl) were counted in the VIGS vector control (-) and *CHUP1*-silenced plants, divided by the total number of chloroplasts, and displayed as percentages. N=12 and 10 for respective columns. (d) Representative Airyscan confocal images of tracked epidermal chloroplasts in response to low (left column) and high (right column) intensity blue light in the VIGS vector control, *CHUP1-, PHOT2-, CHUP1PHOT2-, PHOT1, and CHUP1PHOT1*-silenced plants (see Video 1-4). Chloroplasts tracks are color coded by time and were generated by Imaris spot detection. Purple t=0 seconds (s) and red t=536 seconds. Scale bar = 10 µm. (e) Moving chloroplasts under low (L) and high (H) intensity blue light were counted and divided by the total number of chloroplasts per image and displayed as percentages from the vector control, *PHOT2-, PHOT1-, CHUP1-, CHUP1PHOT2-, or CHUP1PHOT1*-silenced plants. N=12 for silencing control and N=10 for all other columns. (f) The average chloroplast velocities were quantitated under low (L) and high (H) intensity blue light from the vector control, *PHOT2-, PHOT1-, CHUP1-, CHUP1PHOT2-, or CHUP1PHOT1*-silenced plants. N=418, 540, 326, 337, 458, 545, 276, 347, 340, 277, 528, and 593 respective columns. (g) Moving chloroplasts under low (L) and high (H) intensity blue light were counted and divided by the total number of chloroplasts per image and displayed as percentages from the control Arabidopsis Col-0 and *Atchup1* mutant. N=24 for each column. (h) The average chloroplast velocities were quantitated under low (L) and high (H) intensity blue light from the control Col-0 or *Atchup1* mutant. N=438, 533, 543 and 526 for respective columns. For each treatment presented in a, b, and d-h, between 8 to 12 plants were analyzed and one excised leaf sample was analyzed per plant. For each treatment in g and h, 21-24 plants were analyzed and one excised leaf sample was analyzed per plant. In b, e the chloroplast movement was quantitated using Imaris tracking software. In h and j chloroplast movement was tracked by Fiji manual tracking plugin. Data in a,c,d and g were counted manually. In a, b, d-c, the data is displayed as the mean $\pm$ SEM. In a, c, e, g, statistical analysis was conducted on ratios and then converted to percentages for display. Statistically significant difference determined by a Student's t-test with Welch's correction (a, c) or by a Mann-Whitney test (b). Groups were analyzed between low light and high light treatment (e, f), as well as paired analysis within silencing conditions, determined by a Welch's ANOVA with Dunnett's T3 multiple comparison test (e) or a Kruskal-Wallis test with Dunn's multiple comparison test (f). Statistical significance for g and h was determined by a Kruskal-Wallis test with Dunn's multiple comparisons test. Different letters signify significant difference ($p<0.05$). * = $p<0.05$, ** = $p<0.01$, *** = $p<0.001$ and **** = $p<0.0001$.

Fig. 2. Light-induced cp-actin detected on mesophyll but not epidermal chloroplasts.
Nicotiana benthamiana leaves expressing the chloroplast transit peptide (cTP) of RBCS1a fused to mNeonGreen (RBCS1a$_{cTP}$-mNG; green) and actin marker Lifeact-tagRFP (magenta) were imaged by

spinning disk confocal microscopy. (a) Epidermal chloroplasts were exposed to high intensity blue light and three chloroplasts were manually tracked (white lines). (b) Enlarged image of boxed region in (a). Chloroplast associated actin (cp-actin) was not detected on the leading edge of a moving chloroplast (arrowhead). Cp-actin was not detected on a leading small protrusion (bottom arrow) or near the base of a stromule (top arrow) guiding stromule directed movement (SDM). (c) Mesophyll chloroplasts were exposed to the same amount of high intensity blue light as in a, b in order to induce chloroplast movement. Chloroplasts moved from the periclinal position towards the anticlinal position and three chloroplasts were manually tracked (white line). (d) Enlarged image of boxed region in C. Cp-actin was observed on the leading edge of mesophyll chloroplasts (arrowhead) and on their protrusions (arrows). In a and c, scale bar equals 10 µm. In b and d, scale bar equals 2 µm.

Fig. 3. Chloroplast movement partially correlates with cytoplasmic streaming and is reduced by the inhibition of actin polymerization with cytochalasin D.
(a-d) Free Citrine fluorescent protein was transiently expressed in *N. benthamiana* leaves and imaged under low light and high blue light conditions by spinning disk confocal microscopy. (a-b) White lines show the cumulative manual tracking of chloroplasts (red) over 270 seconds (s) in relation to the front of cytoplasmic streams (light cyan line) marked with Citrine (yellow). (a) Chloroplast movement and cytoplasmic streaming in plants without silencing under low light (left panel) and high light (right panels). (b) In a *CHUP1*-silenced plant, a chloroplast was observed moving with a cytoplasmic stream, pulling away from the cytoplasmic stream (arrow) and then moving independently of cytoplasmic streaming. (c) Representative maximum intensity projections of confocal z-stacks of the cytoplasm of the virus-induced gene silencing (VIGS) control or VIGS *CHUP1* plants after treatment with the 0.1% DMSO control or 10 µM cytochalasin D. White arrowheads indicate some of the cytoplasmic streams. (d) Percent of moving chloroplast in VIGS control (-) or *CHUP1*-silenced *N. benthamiana* plants after treatment. N=11 plants for each combination of treatment and VIGS. (e) Percent of moving chloroplasts in Col-0 or *chup1* Arabidopsis plants after treatment. N=8 plants used for each combination of treatment and plant line. (d,e) One image was taken per plant and N equals the number of plants over two experimental replicates. Data is displayed as the mean $\pm$ SEM. Statistical analysis was conducted on ratios and then converted to percentages for display. Statistical significance is determined by a Welch's ANOVA with Dunnett's T3 multiple comparison test between data sets with the same inhibitor treatment. Different letters signify significant difference ($p<0.05$).

Fig. 4. Silencing *CHUP1* induces stromule amount, velocity, and length. (a) Representative Airyscan confocal images of epidermal chloroplast stromules (red arrowheads) marked with the chloroplast transit peptide (cTP) of RBCS1a fused to mNeonGreen ($RBCS1a_{cTP}$-mNG) in the virus-induced gene silencing (VIGS) vector control and *CHUP1*-silenced *Nicotiana benthamiana* plants. Scale bar = 10 µm. (b) The number of stromules was normalized to the number of chloroplasts per image and displayed as a ratio of stromules to chloroplasts in the vector control and *CHUP1*-silenced plants, N=12 and 10 for respective columns. (c-d) Stromule directed movement (SDM) was calculated as correlated movement (>0.6) between the angle of chloroplast movement and the angle of the stromule. SDM counts were normalized to the number of total movement events of chloroplasts with stromules, N=12 and N=10 for respective columns (c) or the total number of moving chloroplasts, N=11 (d), and displayed as percentages. (e) The stromule tip velocity was tracked and quantitated for each stromule, N=689 and 487 for respective columns. (f) The maximum length was calculated for individual stromule during the time lapse datasets from VIGS vector control (-) and *CHUP1*-silenced plants N=688 and 171 for

respective columns. (g) The maximum change in length for individual stromule during a single time point in VIGS vector control (-) and *CHUP1*-silenced plants, N=686 and 486. For each treatment presented in the Fig., between 8 to 12 plants were analyzed and one excised leaf sample was analyzed per plant. Data in b were counted manually. Stromule movement in c-g was calculated using a custom MATLAB tracking program. In b-g, the data is displayed as the mean ± SEM. In, c-d, statistical analysis was conducted on ratios and then converted to percentages for display. Statistically significant difference determined by a Student's t-test with Welch's correction (b, c, d) or by a Mann-Whitney test (e-g). * = $p<0.05$, ** = $p<0.01$, *** = $p<0.001$, **** = $p<0.0001$, and ns = no significance.

Fig. 5. Silencing *CHUP1* auto-activates chloroplast associated innate immune responses. All the experiments were conducted in leaf epidermal cells of transgenic *Nicotiana benthamiana* with N nucleotide-binding leucine-rich repeat (*NLR*) immune receptor except in (e). Effector-triggered immunity (ETI) was induced using the p50 effector from *Tobacco mosaic virus* (TMV-p50). (a) The number of stromules was normalized to the number of chloroplasts per image and displayed as a ratio of stromules to chloroplasts in the virus-induced gene silencing (VIGS) vector control (-) and *CHUP1*-silenced plants with (+) and without (-) ETI induction, N= 13, 16, 16 and 12 for each respective column. (b) The stromule tip velocity was tracked and quantitated for each stromule in the vector control (-) and *CHUP1*-silenced plants with (+) and without (-) ETI induction, N=171, 254, 328 and 225 for each respective column. (c) The maximum length was calculated for each individual stromule during the time lapse datasets from VIGS vector control (-) and *CHUP1*-silenced plants with (+) and without (-) ETI induction, N=563, 625, 803 and 541 for each respective column. (d) The maximum change in length for each individual stromule during a single time point in VIGS vector control (-) and *CHUP1*-silenced plants with (+) and without (-) ETI induction, N=563, 625, 802 and 541. (e) Representative confocal microscopy images showing perinuclear chloroplast clustering in vector control (-) and *CHUP1*-silenced transgenic *N. benthamiana* plants expressing chloroplast stroma marker, NRIP1-Cerulean. Red arrowheads point to the nuclei. Scale bar = 10 µm. (f) The number of chloroplasts surrounding the nucleus were counted in the VIGS vector control (-) and *CHUP1*-silenced plants with (+) and without (-) ETI induction. In a-d, two samples were analyzed per plant for 5 plants for each combination of treatment. In a-d, f, the data is displayed as mean ± SEM. Different letters signify significant difference ($p<0.05$) determined by Brown-Forsythe and Welch's ANOVA tests with Dunnette's T3 multiple comparisons test (a, f) or Kruskal-Wallis test ($p<0.05$) with Dunn's multiple comparison test (b, c, d). p50-HA was used to induced ETI for all data, at 24 hours for a-d while at 30 hours for f.

Fig. 6. Epidermal chloroplast response is induced during ETI and by *CHUP1* silencing. (a) Representative images for epidermal chloroplast response (ECR) in virus-induced gene silencing (VIGS) vector control (-) and *CHUP1*-silenced *Nicotiana benthamiana* plants. Effector-triggered immunity (ETI) using the p50 effector from *Tobacco mosaic virus* (TMV-p50) for 30 hours. Confocal microscopy of chloroplasts autofluorescence (red) was used to determine their position and then overlaid on transmitted light images for display (grayscale). Cells walls are marked with black dashed lines and cells with ECR (yellow text) or no ECR (black text) are labeled. Scale bar equals 20 µm. (b) ECR was quantitated by calculating the percentage of epidermal pavement cells which contain chloroplasts at the surface of the leaf from images shown in A. 2 leaf sample were imaged between 4 plants for each treatment over two experimental replicates, N=41, 40, 37 and 40 for each respective column. (c) Moving chloroplasts were counted and divided against the total number of chloroplasts per image in vector control (-) and *CHUP1*-

738 silenced plants with (+) and without (-) ETI induction. N=13, 16, 16, and 12 for each respective column
739 (d) The chloroplast body velocities in vector control (-) and *CHUP1*-silenced plants were tracked and
740 quantitated with (+) and without (-) ETI induction. N=349, 329, 334, and 280. In c, d two samples were
741 analyzed per plant for 9 and 5 plants respectively for each combination of conditions. In b, c, statistical
742 analysis was conducted on ratios and then converted to percentages for display. In b, c, and d, the data
743 is displayed as mean ± SEM. Different letters signify significant difference ($p<0.05$) determined by
744 Brown-Forsythe and Welch's ANOVA tests with Dunnette's T3 multiple comparisons test (b, c) or
745 Kruskal-Wallis test ($p<0.05$) with Dunn's multiple comparison test (d). p50-HA was used to induce ETI for
746 all data at 30 hours for a, b and at 24 hours for c, d.
747
748 **Fig. 7. Hydrogen peroxide is required for enhanced PCD in *CHUP1*-silenced plants.** The chloroplast
749 transit peptide of RBCS1a was fused to the hydrogen peroxide (H_2O_2) sensor HyPer7 (RBCS1a$_{cTP}$-HyPer7),
750 mKate2-tagged ascorbate peroxidase (cTP-APX-mKate2), or the control mKate2 (cTP-mKate2) and
751 transiently expressed in *Nicotiana benthamiana* with N nucleotide-binding leucine-rich repeat (*NLR*)
752 immune receptor. H_2O_2 levels were measured as the ratio of RBCS1a$_{cTP}$-HyPer7 fluorescence excited
753 with 488 nm or 405 nm laser light on a confocal microscope. RBCS1a$_{cTP}$ abbreviated to cTP in graphs.
754 Effector-triggered immunity (ETI) was induced using the p50 effector from *Tobacco mosaic virus* (TMV-
755 p50). (a) Representative ratiometric images of H_2O_2 levels detected by RBCS1a$_{cTP}$-HyPer7 in epidermal
756 chloroplasts of the virus-induced gene silencing (VIGS) control and *CHUP1*-silenced plants with and
757 without ETI induction. Scale equals 20 µm. (a-c) For two experimental replicates, ratiometric HyPer7
758 measurements of H_2O_2 in VIGS silencing control (-) and *CHUP1*-silenced plants with (+) and without ETI (-
759) induction and either with the RBCS1a$_{cTP}$-mKate2 control, N=2872, 1843, 2649 and 2563, (b) or
760 RBCS1a$_{cTP}$-APX-mKate2, N=2933, 1838, 2893 and 1585 (c). ETI was induced using XVE::p50-tRFP using 30
761 µM estradiol for six hours (h). 10-20 images were collected for six plants in one experiment. (d-e) ETI-
762 induced cell death was quantitated by measuring the conductivity of ion leakage from leaf tissue.
763 Conductivity measurements were taken from leaf samples of VIGS vector control and *CHUP1*-silenced
764 plants with and without ETI induction and either with the RBCS1a$_{cTP}$-mKate2 control (d) or RBCS1a$_{cTP}$-
765 APX-mKate2 (e). ETI was induced with XVE::p50-3xHA in two different plants with three leaf sections
766 from each, N=6. In b and c, data is displayed as the mean ± SEM. In d and e, data is displayed as the
767 mean at each time point. Different letters signify significant difference ($p<0.05$) determined by Kruskal-
768 Wallis test ($p<0.05$) with Dunn's multiple comparison test.
769
770 **Fig. 8. Hydrogen peroxide is required for stromule induction but not chloroplast movement.** The
771 chloroplast transit peptide of RBCS1a was fused to the hydrogen peroxide (H_2O_2) sensor HyPer7
772 (RBCS1a$_{cTP}$-HyPer7) or mKate2-tagged ascorbate peroxidase (cTP-APX), or the control mKate2 (cTP-
773 mKate2) and transiently expressed in *Nicotiana benthamiana* with N NLR immune receptor. Effector-
774 triggered immunity (ETI) was induced using the p50 effector from *Tobacco mosaic virus* (TMV-p50). (a)
775 The number of stromules was normalized to the number of chloroplasts per image and displayed as a
776 ratio of stromules to chloroplasts in the virus-induced gene silencing (VIGS) vector control (-) and
777 *CHUP1*-silenced *N. benthamiana* plants with (+) or without (-) ETI induction and with (+) or without (-)
778 RBCS1a$_{cTP}$-APX-mKate2, N=26, 24, 22, 22, 29, 22, 27 and 25 for each respective column. (b) In plants
779 transiently expressing HyPer7, hydrogen peroxide (H_2O_2) was induced with a high laser intensity ($28\ \mu W$)
780 on a confocal microscope, and changes in H_2O_2 were quantitated over 10 minutes (min) with ratiometric
781 HyPer7 measurements. Line graph showing changes in ratiometric HyPer7 measurements of H_2O_2

accumulation by high intensity light in the VIGS vector control (-) and *CHUP1*-silenced plants with ETI (+ETI) or without ETI (-Control) induction and with the RBCS1a$_{cTP}$-mKate2 expression control (solid lines), N=5, or RBCS1a$_{cTP}$-APX-mKate2 (dashed lines), N=2. Colored arrows indicate peaks of matching color lines. (c-d) The number of moving chloroplasts (c) and stromules (d) was normalized to the number of chloroplasts per image and displayed as percentage (c) or a ratio (d). These measurements were made in the VIGS vector control (-) and *CHUP1*-silenced plants with low (L) or (H) high intensity blue light induction and with (+) or without (-) RBCS1a$_{cTP}$-APX. Statistical analysis was performed between shared silencing treatment and light treatments, N=20, 20, 19, 19, 13, 13, 18 and 18 for each column. For a, c and d, data is displayed as the mean $\pm$ SEM. For b, data is displayed as the mean for each time point. Different letters signify significant difference ($p<0.05$) determined by Brown-Forsythe and Welch's ANOVA tests with Dunnette's T3 multiple comparisons test.

Video Legends

Video 1. Montage of light induced chloroplast movement in *CHUP1, PHOT2, and CHUP1PHOT2* silenced plants. Chloroplast movement with low and high light levels. The montage shows side-by-side comparison of all chloroplast movement in the VIGS and light treatments shown in Fig. 1c and Videos 1-3. The chloroplast transit peptide of RBCS1a was fused to mNeonGreen (RBCS1a$_{cTP}$-mNG) and transiently expressed in *Nicotiana benthamiana* plants. RBCS1a$_{cTP}$-mNG expressing chloroplast (grey) were identified with Imaris spot detection and tracks are color coded by time. Scale bar = 10 µm.

Video 2. High blue light induced movement. Chloroplast movement under low and high levels of blue light. Final time point shown in Fig. 1c, column 1. The chloroplast transit peptide of RBCS1a was fused to mNeonGreen (RBCS1a$_{cTP}$-mNG) and transiently expressed in *Nicotiana benthamiana* plants. RBCS1a$_{cTP}$-mNG expressing chloroplast (grey) were identified with Imaris spot detection and tracks are color coded by time. Scale bar = 10 µm.

Video 3. *CHUP1* silencing phenotype. *CHUP1*-silenced plants have increased chloroplast movement under low and high levels of blue light. The chloroplast transit peptide of RBCS1a was fused to mNeonGreen (RBCS1a$_{cTP}$-mNG) and transiently expressed in *Nicotiana benthamiana* plants. RBCS1a$_{cTP}$-mNG expressing chloroplast (grey) were identified with Imaris spot detection and tracks are color coded by time. Scale bar = 10 µm.

Video 4. *PHOT1* and *CHUP1PHOT2* silencing phenotype. Chloroplast movement under high levels of blue light showing the loss light induced movement in *PHOT2*-silenced and restoration of movement *CHUP1PHOT2-s*ilenced *Nicotiana benthamiana* plants*.* The chloroplast transit peptide of RBCS1a was fused to mNeonGreen (RBCS1a$_{cTP}$-mNG) and transiently expressed in *N. benthamiana* plants. RBCS1a$_{cTP}$-mNG expressing chloroplast (grey) were identified with Imaris spot detection and tracks are color coded by time. Scale bar = 10 µm.

Video 5. Blue light induced chloroplast movement in epidermal and mesophyll cells. *Nicotiana benthamiana* leaves expressing RBCS1a$_{cTP}$-mNG (green) and actin marker Lifeact-tagRFP (magenta) were imaged on a spinning disk confocal microscope. Chloroplasts were manually tracked (white lines) in epidermal cells for 10 minutes (min) and mesophyll cells for 17 minutes. Scale bar = 10 µm.

Video 6. Blue light induced chloroplast movement in epidermal and mesophyll cell of the same leaf section. *Nicotiana benthamiana* leaves expressing RBCS1a$_{cTP}$-mNG (green) and actin marker Lifeact-tagRFP (magenta) were imaged on a spinning disk confocal microscope. Magnified views of the boxed area (yellow) are shown on the left. Epidermal chloroplasts were manually tracked (white lines) for 10 minutes (min). Scale bar = 10 µm.

Video 7. Blue light induced chloroplast movement with mTalin marked actin. *Nicotiana benthamiana* leaves expressing mTalin-GFP (green) were imaged on a spinning disk confocal microscope. Scale bar = 20 µm. Magnified view of chloroplasts (red), mTalin (green), and the overlay. Chloroplasts were manually tracked (white lines). Time lapse is 270 seconds (sec) long and repeated four times for clarity. Scale bar = 2 µm.

Video 8. Cytoplasmic streaming in wild-type *N. benthamiana*. *Nicotiana benthamiana* leaves expressing free Citrine (yellow) were imaged on a spinning disk confocal microscope. A time lapse dataset using low light was first acquired, followed by a time lapse dataset using high blue light. Time

lapse datasets are 270 seconds (sec) long and repeated twice for clarity. White boxed areas designate the magnified views. Scale bar = 20 µm in overview videos and 2 µm in magnified views.

Video 9. Cytoplasmic streaming in *CHUP1*-silenced *N. benthamiana*. Free Citrine (yellow) was expressed in virus-induced gene silencing (VIGS) control and *CHUP1*-silenced *N. benthamiana* plants and imaged on a spinning disk confocal microscope. 1 hour prior to imaging, plants were infiltrated with either a DMSO control or 10 µM cytochalasin D. A time lapse dataset using low light was first acquired, followed by a time lapse dataset using high blue light. Time lapse datasets are 270 seconds long and repeated twice for clarity. White boxed areas designate the magnified views. Scale bar = 20 µm in overview videos and 2 µm in magnified views.

Video 10. Cytoplasmic streaming in Arabidopsis Col-0 and *atchup1* mutants. Col-0 and *atchup1* leaves were infiltrated with CMFDA tracer dye to mark the cytoplasm and imaged on a spinning disk confocal microscope. 1 hour prior to imaging, plants were infiltrated with either a DMSO control or 10 µM cytochalasin D. A time lapse dataset using low light was first acquired, followed by a time lapse dataset using high blue light. Time lapse datasets are 270 seconds (sec) long. Scale bar = 20 µm.

Video 11. Light induced ROS during ETI. The chloroplast transit peptide of RBCS1a was fused to the H_2O_2 sensor HyPer7 (RBCS1a$_{cTP}$-HyPer7) and transiently expressed in *Nicotiana benthamiana* with N nucleotide binding leucine rich repeat (NLR) immune receptor. Ratiometric videos of H_2O_2 levels detected by RBCS1a$_{cTP}$-HyPer7 in epidermal chloroplasts of the VIGS silencing control and *CHUP1*-silenced plants with and without effector-triggered immunity (ETI) induction and with and without ascorbate peroxidase (APX). Time lapse datasets are 198 seconds (sec) long. Scale bar = 20 µm.

References

Andersson B, Anderson JM. 1980. Lateral Heterogeneity in the Distribution of Chlorophyll-Protein Complexes of the Thylakoid Membranes of Spinach-Chloroplasts. *Biochimica Et Biophysica Acta* **593**(2): 427-440.

Avisar D, Prokhnevsky AI, Makarova KS, Koonin EV, Dolja VV. 2008. Myosin XI-K Is required for rapid trafficking of Golgi stacks, peroxisomes, and mitochondria in leaf cells of Nicotiana benthamiana. *Plant Physiol* **146**(3): 1098-1108.

Badawi GH, Kawano N, Yamauchi Y, Shimada E, Sasaki R, Kubo A, Tanaka K. 2004. Over-expression of ascorbate peroxidase in tobacco chloroplasts enhances the tolerance to salt stress and water deficit. *Physiologia Plantarum* **121**(2): 231-238.

Balint-Kurti P. 2019. The plant hypersensitive response: concepts, control and consequences. *Mol Plant Pathol* **20**(8): 1163-1178.

Barton KA, Schattat MH, Jakob T, Hause G, Wilhelm C, McKenna JF, Mathe C, Runions J, Van Damme D, Mathur J. 2016. Epidermal Pavement Cells of Arabidopsis Have Chloroplasts. *Plant Physiol* **171**(2): 723-726.

Beltran J, Wamboldt Y, Sanchez R, LaBrant EW, Kundariya H, Virdi KS, Elowsky C, Mackenzie SA. 2018. Specialized Plastids Trigger Tissue-Specific Signaling for Systemic Stress Response in Plants. *Plant Physiol* **178**(2): 672-683.

Brunkard JO, Runkel AM, Zambryski PC. 2015. Chloroplasts extend stromules independently and in response to internal redox signals. *Proceedings of the National Academy of Sciences* **112**(32): 10044-10049.

Cai C, Henty-Ridilla JL, Szymanski DB, Staiger CJ. 2014. Arabidopsis myosin XI: a motor rules the tracks. *Plant Physiol* **166**(3): 1359-1370.

Caplan L, Jeffrey, Kumar S, Amutha, Park E, Padmanabhan S, Meenu, Hoban K, Modla S, Czymmek K, Dinesh-Kumar P, Savithramma. 2015. Chloroplast Stromules Function during Innate Immunity. *Developmental Cell* **34**(1): 45-57.

Caplan L, Jeffrey, Mamillapalli P, Burch-Smith TM, Czymmek K, Dinesh-Kumar SP. 2008. Chloroplastic Protein NRIP1 Mediates Innate Immune Receptor Recognition of a Viral Effector. *Cell* **132**(3): 449-462.

de Souza A, Wang JZ, Dehesh K. 2017. Retrograde Signals: Integrators of Interorganellar Communication and Orchestrators of Plant Development. *Annu Rev Plant Biol* **68**: 85-108.

DeBlasio SL, Luesse DL, Hangarter RP. 2005. A plant-specific protein essential for blue-light-induced chloroplast movements. *Plant Physiol* **139**(1): 101-114.

Dinesh-Kumar SP, Anandalakshmi R, Marathe R, Schiff M, Liu Y 2003. Virus-induced Gene Silencing. *Plant Functional Genomics*. Methods in Molecular Biology: Humana Press, 287-294.

Ding X, Jimenez-Gongora T, Krenz B, Lozano-Duran R. 2019. Chloroplast clustering around the nucleus is a general response to pathogen perception in Nicotiana benthamiana. *Mol Plant Pathol* **20**(9): 1298-1306.

Dong XJ, Ryu JH, Takagi S, Nagai R. 1996. Dynamic changes in the organization of microfilaments associated with the photocontrolled motility of chloroplasts in epidermal cells of Vallisneria. *Protoplasma* **195**(1-4): 18-24.

Dopp IJ, Kalac K, Mackenzie SA. 2023. Hydrogen peroxide sensor HyPer7 illuminates tissue-specific plastid redox dynamics. *Plant Physiology* **193**(1): 217-228.

Dopp IJ, Yang X, Mackenzie SA. 2021. A new take on organelle-mediated stress sensing in plants. *New Phytologist* **230**(6): 2148-2153.

Dwyer ME, Hangarter RP. 2021. Light-dependent phosphorylation of THRUMIN1 regulates its association with actin filaments and 14-3-3 proteins. *Plant Physiology* **187**(3): 1445-1461.

Dwyer ME, Hangarter RP. 2022. Light-induced displacement of PLASTID MOVEMENT IMPAIRED1 precedes light-dependent chloroplast movements. *Plant Physiol* **189**(3): 1866-1880.

Dyachok J, Sparks JA, Liao F, Wang YS, Blancaflor EB. 2014. Fluorescent protein-based reporters of the actin cytoskeleton in living plant cells: fluorophore variant, actin binding domain, and promoter considerations. *Cytoskeleton (Hoboken)* **71**(5): 311-327.

Exposito-Rodriguez M, Laissue PP, Yvon-Durocher G, Smirnoff N, Mullineaux PM. 2017. Photosynthesis-dependent H(2)O(2) transfer from chloroplasts to nuclei provides a high-light signalling mechanism. *Nat Commun* **8**(1): 49.

Foissner I, Wasteneys GO. 2007. Wide-Ranging Effects of Eight Cytochalasins and Latrunculin A and B on Intracellular Motility and Actin Filament Reorganization in Characean Internodal Cells. *Plant and Cell Physiology* **48**(4): 585-597.

Gotoh E, Suetsugu N, Yamori W, Ishishita K, Kiyabu R, Fukuda M, Higa T, Shirouchi B, Wada M. 2018. Chloroplast Accumulation Response Enhances Leaf Photosynthesis and Plant Biomass Production. *Plant Physiol* **178**(3): 1358-1369.

Gray JC, Hansen MR, Shaw DJ, Graham K, Dale R, Smallman P, Natesan SK, Newell CA. 2012. Plastid stromules are induced by stress treatments acting through abscisic acid. *Plant Journal* **69**: 387-398.

Hatsugai N, Katagiri F. 2018. Quantification of Plant Cell Death by Electrolyte Leakage Assay. *Bio Protoc* **8**(5): e2758.

Higa T, Suetsugu N, Kong S-G, Wada M. 2014. Actin-dependent plastid movement is required for motive force generation in directional nuclear movement in plants. *Proceedings of the National Academy of Sciences* **111**(11): 4327-4331.

Holzinger A, Blaas K. 2016. Actin-Dynamics in Plant Cells: The Function of Actin-Perturbing Substances: Jasplakinolide, Chondramides, Phalloidin, Cytochalasins, and Latrunculins. *Methods Mol Biol* **1365**: 243-261.

Ichikawa S, Yamada N, Suetsugu N, Wada M, Kadota A. 2011. Red light, Phot1 and JAC1 modulate Phot2-dependent reorganization of chloroplast actin filaments and chloroplast avoidance movement. *Plant Cell Physiol* **52**(8): 1422-1432.

Irieda H. 2022. Emerging Roles of Motile Epidermal Chloroplasts in Plant Immunity. *International Journal of Molecular Sciences* **23**(7).

Irieda H, Takano Y. 2021. Epidermal chloroplasts are defense-related motile organelles equipped with plant immune components. *Nat Commun* **12**(1): 2739.

Ishishita K, Higa T, Tanaka H, Inoue SI, Chung A, Ushijima T, Matsushita T, Kinoshita T, Nakai M, Wada M, et al. 2020. Phototropin2 Contributes to the Chloroplast Avoidance Response at the Chloroplast-Plasma Membrane Interface. *Plant Physiol* **183**(1): 304-316.

Jarillo JA, Gabrys H, Capel J, Alonso JM, Ecker JR, Cashmore AR. 2001. Phototropin-related NPL1 controls chloroplast relocation induced by blue light. *Nature* **410**(6831): 952-954.

Jwa NS, Hwang BK. 2017. Convergent Evolution of Pathogen Effectors toward Reactive Oxygen Species Signaling Networks in Plants. *Front Plant Sci* **8**: 1687.

Kachroo P, Burch-Smith TM, Grant M. 2021. An Emerging Role for Chloroplasts in Disease and Defense. *Annu Rev Phytopathol* **59**: 423-445.

Kadota A, Yamada N, Suetsugu N, Hirose M, Saito C, Shoda K, Ichikawa S, Kagawa T, Nakano A, Wada M. 2009. Short actin-based mechanism for light-directed chloroplast movement in *Arabidopsis*. *Proceedings of the National Academy of Sciences* **106**(31): 13106-13111.

Kagawa T, Sakai T, Suetsugu N, Oikawa K, Ishiguro S, Kato T, Tabata S, Okada K, Wada M. 2001. Arabidopsis NPL1: a phototropin homolog controlling the chloroplast high-light avoidance response. *Science* **291**(5511): 2138-2141.

Kagawa T, Wada M. 2002. Blue light-induced chloroplast relocation. *Plant Cell Physiol* **43**(4): 367-371.

Kasahara M, Kagawa T, Oikawa K, Suetsugu N, Miyao M, Wada M. 2002. Chloroplast avoidance movement reduces photodamage in plants. *Nature* **420**(6917): 829-832.

Ketelaar T, Anthony RG, Hussey PJ. 2004. Green Fluorescent Protein-mTalin Causes Defects in Actin Organization and Cell Expansion in Arabidopsis and Inhibits Actin Depolymerizing Factor's Actin Depolymerizing Activity in Vitro. *Plant Physiology* **136**(4): 3990-3998.

Kinoshita T, Doi M, Suetsugu N, Kagawa T, Wada M, Shimazaki K. 2001. Phot1 and phot2 mediate blue light regulation of stomatal opening. *Nature* **414**(6864): 656-660.

Kong S-G, Arai Y, Suetsugu N, Yanagida T, Wada M. 2013. Rapid Severing and Motility of Chloroplast-Actin Filaments Are Required for the Chloroplast Avoidance Response in Arabidopsis *The Plant Cell* **25**(2): 572-590.

Kong SG, Yamazaki Y, Shimada A, Kijima ST, Hirose K, Katoh K, Ahn J, Song HG, Han JW, Higa T, et al. 2024. CHLOROPLAST UNUSUAL POSITIONING 1 is a plant-specific actin polymerization factor regulating chloroplast movement. *Plant Cell* **36**(4): 1159-1181.

Kumar AS, Park E, Nedo A, Alqarni A, Ren L, Hoban K, Modla S, McDonald JH, Kambhamettu C, Dinesh-Kumar SP, et al. 2018. Stromule extension along microtubules coordinated with actin-mediated anchoring guides perinuclear chloroplast movement during innate immunity. *eLife* **7**: e23625.

Kunz J, Ullmann T, Kneisel C, Baumhauer R. 2023. Three-dimensional subsurface architecture and its influence on the spatiotemporal development of a retrogressive thaw slump in the Richardson Mountains, Northwest Territories, Canada. *Arctic Antarctic and Alpine Research* **55**(1).

Łabuz J, Sztatelman O, Hermanowicz P. 2022. Molecular insights into the phototropin control of chloroplast movements. *Journal of Experimental Botany* **73**(18): 6034-6051.

Liu Y, Ren D, Pike S, Pallardy S, Gassmann W, Zhang S. 2007. Chloroplast-generated reactive oxygen species are involved in hypersensitive response-like cell death mediated by a mitogen-activated protein kinase cascade. *Plant Journal* **51**(6): 941-954.

Liu Y, Schiff M, Marathe R, Dinesh-Kumar SP. 2002. Tobacco Rar1, EDS1 and NPR1/NIM1 like genes are required for N-mediated resistance to tobacco mosaic virus. *Plant Journal* **30**(4): 415-429.

Lowe DG. 2004. Distinctive image features from scale-invariant keypoints. *International Journal of Computer Vision* **60**(2): 91-110.

Luesse DR, DeBlasio SL, Hangarter RP. 2010. Integration of Phot1, Phot2, and PhyB signalling in light-induced chloroplast movements. *Journal of Experimental Botany* **61**(15): 4387-4397.

Meier ND, Seward K, Caplan JL, Dinesh-Kumar SP. 2023. Calponin-homology domain containing kinesin, KIS1, regulates chloroplast stromule formation and immunity. *Science Advances* **In press**.

Montes-Rodriguez A, Kost B. 2017. Direct Comparison of the Performance of Commonly Employed In Vivo F-actin Markers (Lifeact-YFP, YFP-mTn and YFP-FABD2) in Tobacco Pollen Tubes. *Frontiers in Plant Science* **8**.

Mustárdy L, Garab G. 2003. Granum revisited.: A three-dimensional model -: where things fall into place. *Trends in Plant Science* **8**(3): 117-122.

Natesan SKA, Sullivan JA, Gray JC. 2009. Myosin XI Is Required for Actin-Associated Movement of Plastid Stromules. *Molecular Plant* **2**(6): 1262-1272.

Oikawa K, Kasahara M, Kiyosue T, Kagawa T, Suetsugu N, Takahashi F, Kanegae T, Niwa Y, Kadota A, Wada M. 2003. Chloroplast unusual positioning1 is essential for proper chloroplast positioning. *Plant Cell* **15**(12): 2805-2815.

Oikawa K, Yamasato A, Kong SG, Kasahara M, Nakai M, Takahashi F, Ogura Y, Kagawa T, Wada M. 2008. Chloroplast outer envelope protein CHUP1 is essential for chloroplast anchorage to the plasma membrane and chloroplast movement. *Plant Physiol* **148**(2): 829-842.

Pak VV, Ezeriņa D, Lyublinskaya OG, Pedre B, Tyurin-Kuzmin PA, Mishina NM, Thauvin M, Young D, Wahni K, Martínez Gache SA, et al. 2020. Ultrasensitive Genetically Encoded Indicator for Hydrogen Peroxide Identifies Roles for the Oxidant in Cell Migration and Mitochondrial Function. *Cell Metabolism* **31**(3): 642-653.e646.

Panstruga R, Moscou MJ. 2020. What is the Molecular Basis of Nonhost Resistance? *Molecular Plant-Microbe Interactions®* **33**(11): 1253-1264.

Park E, Nedo A, Caplan JL, Dinesh-Kumar SP. 2018. Plant-microbe interactions: organelles and the cytoskeleton in action. *New Phytologist* **217**(3): 1012-1028.

Poulsen CP, Vereb G, Geshi N, Schulz A. 2013. Inhibition of cytoplasmic streaming by cytochalasin D is superior to paraformaldehyde fixation for measuring FRET between fluorescent protein-tagged Golgi components. *Cytometry A* **83**(9): 830-838.

Pyke K. 2009. *Plastid biology*: Cambridge University Press.

Pyke K, López-Juez E. 1999. Cellular Differentiation and Leaf Morphogenesis in Arabdopsis. *Critical Reviews in Plant Sciences* **18**(4): 527-546.

Ronneberger O, Fischer P, Brox T. 2015. U-Net: Convolutional Networks for Biomedical Image Segmentation. *Medical Image Computing and Computer-Assisted Intervention, Pt Iii* **9351**: 234-241.

Sakai T, Kagawa T, Kasahara M, Swartz TE, Christie JM, Briggs WR, Wada M, Okada K. 2001. Arabidopsis nph1 and npl1: blue light receptors that mediate both phototropism and chloroplast relocation. *Proc Natl Acad Sci U S A* **98**(12): 6969-6974.

Sakai Y, Takagi S. 2017. Roles of actin cytoskeleton for regulation of chloroplast anchoring. *Plant Signaling & Behavior* **12**(10): e1370163.

Sattarzadeh A, Krahmer J, Germain AD, Hanson MR. 2009. A myosin XI tail domain homologous to the yeast myosin vacuole-binding domain interacts with plastids and stromules in Nicotiana benthamiana. *Mol Plant* **2**(6): 1351-1358.

Savage Z, Duggan C, Toufexi A, Pandey P, Liang Y, Segretin ME, Yuen LH, Gaboriau DCA, Leary AY, Tumtas Y, et al. 2021. Chloroplasts alter their morphology and accumulate at the pathogen interface during infection by *Phytophthora infestans*. *The Plant Journal* **107**(6): 1771-1787.

Schindelin J, Arganda-Carreras I, Frise E, Kaynig V, Longair M, Pietzsch T, Preibisch S, Rueden C, Saalfeld S, Schmid B, et al. 2012. Fiji: an open-source platform for biological-image analysis. *Nat Methods* **9**(7): 676-682.

Shapiguzov A, Vainonen JP, Wrzaczek M, Kangasjarvi J. 2012. ROS-talk - how the apoplast, the chloroplast, and the nucleus get the message through. *Front Plant Sci* **3**: 292.

Suetsugu N, Higa T, Gotoh E, Wada M. 2016. Light-Induced Movements of Chloroplasts and Nuclei Are Regulated in Both Cp-Actin-Filament-Dependent and -Independent Manners in Arabidopsis thaliana. *PLOS ONE* **11**(6): e0157429.

Suetsugu N, Higa T, Kong SG, Wada M. 2015. PLASTID MOVEMENT IMPAIRED1 and PLASTID MOVEMENT IMPAIRED1-RELATED1 Mediate Photorelocation Movements of Both Chloroplasts and Nuclei. *Plant Physiol* **169**(2): 1155-1167.

Suetsugu N, Kagawa T, Wada M. 2005. An auxilin-like J-domain protein, JAC1, regulates phototropin-mediated chloroplast movement in Arabidopsis. *Plant Physiol* **139**(1): 151-162.

Suetsugu N, Sato Y, Tsuboi H, Kasahara M, Imaizumi T, Kagawa T, Hiwatashi Y, Hasebe M, Wada M. 2012. The KAC family of kinesin-like proteins is essential for the association of chloroplasts with the plasma membrane in land plants. *Plant Cell Physiol* **53**(11): 1854-1865.

Suetsugu N, Yamada N, Kagawa T, Yonekura H, Uyeda TQ, Kadota A, Wada M. 2010. Two kinesin-like proteins mediate actin-based chloroplast movement in Arabidopsis thaliana. *Proc Natl Acad Sci U S A* **107**(19): 8860-8865.

Takagi S, Kamitsubo E, Nagai R. 1991. Light-Induced Changes in the Behavior of Chloroplasts under Centrifugation in Vallisneria Epidermal Cells. *Journal of Plant Physiology* **138**(3): 257-262.

Takemiya A, Inoue S, Doi M, Kinoshita T, Shimazaki K. 2005. Phototropins promote plant growth in response to blue light in low light environments. *Plant Cell* **17**(4): 1120-1127.

Tominaga M, Ito K. 2015. The molecular mechanism and physiological role of cytoplasmic streaming. *Current Opinion in Plant Biology* **27**: 104-110.

Torres MA. 2010. ROS in biotic interactions. *Physiol Plant* **138**(4): 414-429.

Trotta A, Rahikainen M, Konert G, Finazzi G, Kangasjarvi S. 2014. Signalling crosstalk in light stress and immune reactions in plants. *Philos Trans R Soc Lond B Biol Sci* **369**(1640): 20130235.

van der Honing HS, van Bezouwen LS, Emons AM, Ketelaar T. 2011. High expression of Lifeact in Arabidopsis thaliana reduces dynamic reorganization of actin filaments but does not affect plant development. *Cytoskeleton (Hoboken)* **68**(10): 578-587.

Wada M, Kong S-G. 2018. Actin-mediated movement of chloroplasts. *Journal of Cell Science* **131**(2): jcs210310.

Wang B, Zhou Z, Zhou JM, Li J. 2024. Myosin XI-mediated BIK1 recruitment to nanodomains facilitates FLS2-BIK1 complex formation during innate immunity in Arabidopsis. *Proc Natl Acad Sci U S A* **121**(25): e2312415121.

Whippo CW, Khurana P, Davis PA, DeBlasio SL, DeSloover D, Staiger CJ, Hangarter RP. 2011. THRUMIN1 is a light-regulated actin-bundling protein involved in chloroplast motility. *Curr Biol* **21**(1): 59-64.

Williamson RE. 1972. A light-microscope study of the action of cytochalasin b on the cells and isolated cytoplasm of the characeae. *Journal of Cell Science* **10**(3): 811-819.

Yabuta Y, Motoki T, Yoshimura K, Takeda T, Ishikawa T, Shigeoka S. 2002. Thylakoid membrane-bound ascorbate peroxidase is a limiting factor of antioxidative systems under photo-oxidative stress. *The Plant Journal* **32**(6): 915-925.

Yang F, Xiao K, Pan H, Liu J. 2021. Chloroplast: The Emerging Battlefield in Plant-Microbe Interactions. *Front Plant Sci* **12**: 637853.

Yang Y, Sage TL, Liu Y, Ahmad TR, Marshall WF, Shiu SH, Froehlich JE, Imre KM, Osteryoung KW. 2011. CLUMPED CHLOROPLASTS 1 is required for plastid separation in Arabidopsis. *Proc Natl Acad Sci U S A* **108**(45): 18530-18535.

Yu X, Feng B, He P, Shan L. 2017. From Chaos to Harmony: Responses and Signaling upon Microbial Pattern Recognition. *Annu Rev Phytopathol* **55**: 109-137.

Zuo J, Niu Q-W, Chua N-H. 2000. An estrogen receptor-based transactivator XVE mediates highly inducible gene expression in transgenic plants. *The Plant Journal* **24**(2): 265-273.

The following Supporting Information is available for this article:

Fig. S1 Knockdown of expression of genes by virus-induced gene silencing.

Fig. S2 *Tobacco rattle virus* characterization in *CHUP1*-silenced *N. benthamiana* plants.

Fig. S3 Red light does not increase chloroplast movement in *CHUP1*-silenced *N. benthamiana* or Arabidopsis *chup1* mutant plants.

1083 **Fig. S4** Chloroplast-associated actin was not detectable during light induced chloroplast movement with
1084 fluorescent protein actin markers.

1085 **Fig. S5** Partial correlation of chloroplast movement with cytoplasmic streaming.

1086 **Fig. S6** Quantification of rapid linear chloroplast movement correlated with cytoplasmic streaming.

1087 **Fig. S7** Types of chloroplast and stromule movement measurements and classifications.

1088 **Fig. S8** Quantitation of stromules during low and high intensity blue light.

1089 **Fig. S9** Frequency of stromule extension and retractions.

1090 **Fig. S10** Examination of the effects of and *PHOT1*-silencing on stromules and chloroplasts movement
1091 during effector-triggered immunity.

1092 **Fig. S11** CHUP1 expression increased during effector-triggered immunity induction.

1093 **Fig. S12** Increase hydrogen peroxide in *CHUP1*-silenced plants is dependent on light.

1094 **Fig. S13** Co-localization of chloroplast-targeted HyPer7 and ascorbate peroxidase.

1095 **Fig. S14** Hydrogen peroxide is required for increased chloroplast movement in *CHUP1*-silenced plants.

1096 **Fig. S15** Light induced hydrogen peroxide during effector-triggered immunity.

1097 **Table S1.** Description of constructs.

1098 **Table S2.** List of primers used in this study.

1099 **Table S3.** Imaging laser power levels.

1100 **Table S4.** Description of metrics.

1101 **Methods S1.** Plant growth conditions.

1102 **Methods S2.** Quantitative real time PCR to assess virus-induced gene silencing efficiency.

1103 **Methods S3.** Image analysis of stromules and chloroplast movement.

1104 **Methods S4.** Actin inhibitor treatments.

1105 **Methods S5.** Measurement of cell death by conductivity assay.

1106 **Note S1.** Interpretation of data using actin markers.

1107

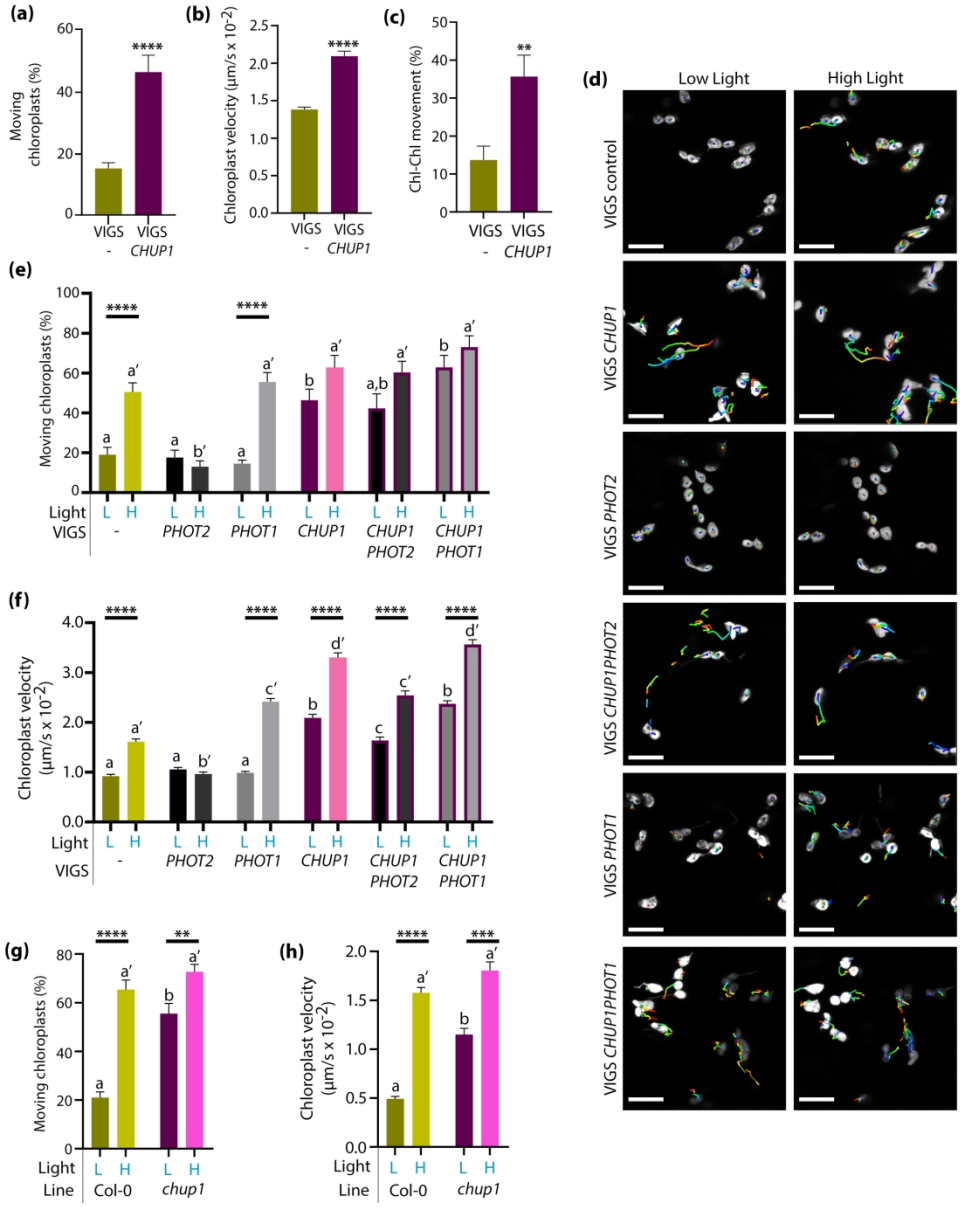

Fig. 1. Silencing CHUP1 increases epidermal chloroplast movement.

194x243mm (300 x 300 DPI)

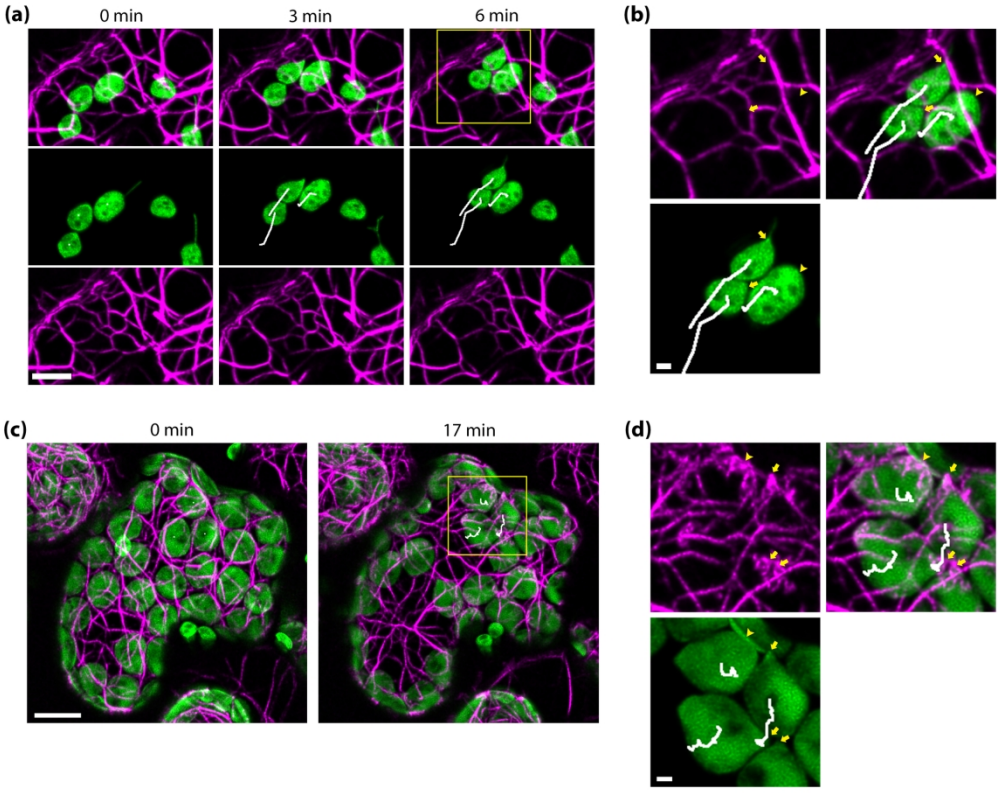

Fig. 2. Light-induced cp-actin detected on mesophyll but not epidermal chloroplasts.

188x149mm (300 x 300 DPI)

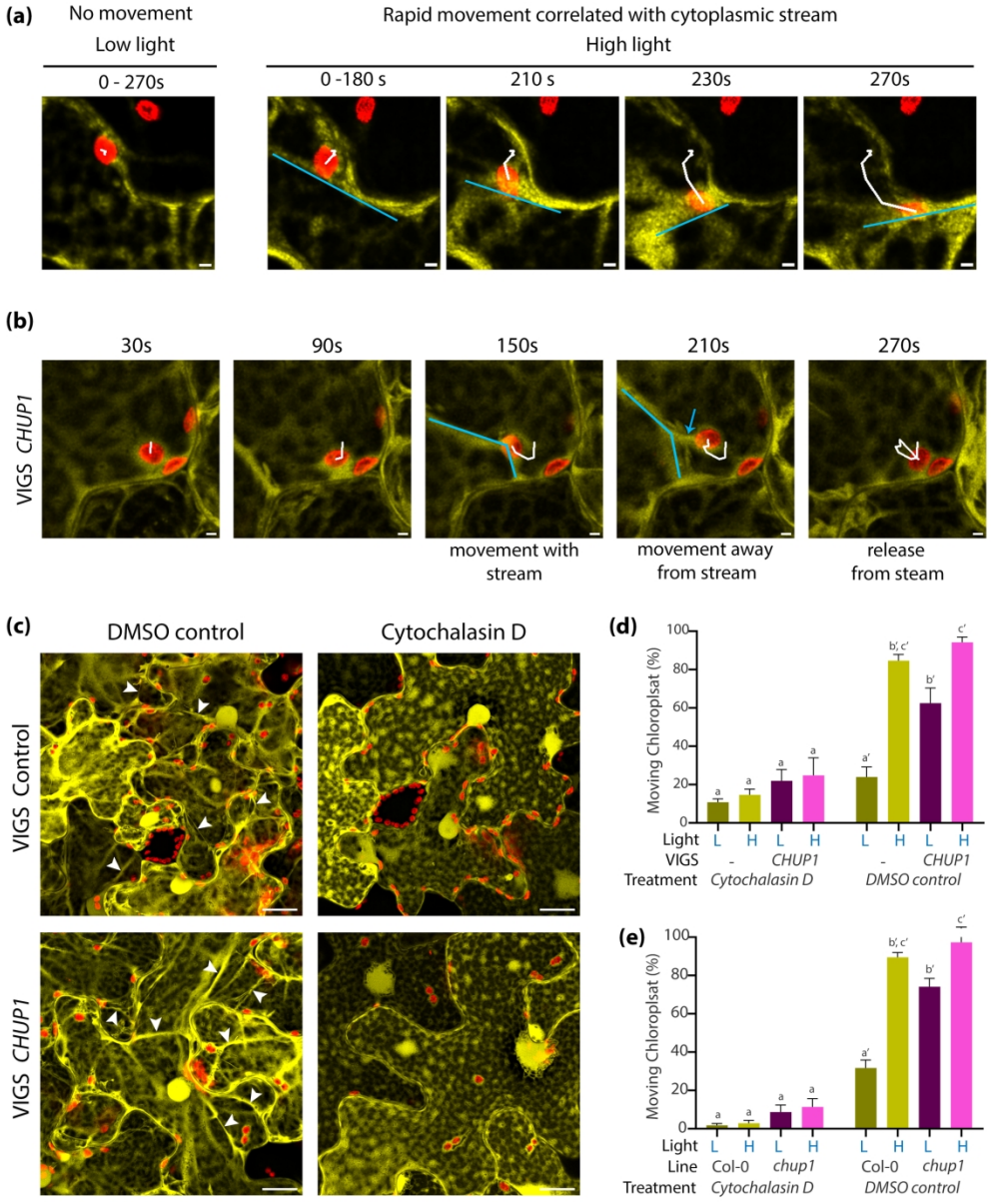

Fig. 3. Chloroplast movement partially correlates with cytoplasmic streaming and is reduced by the inhibition of actin polymerization with cytochalasin D.

177x215mm (300 x 300 DPI)

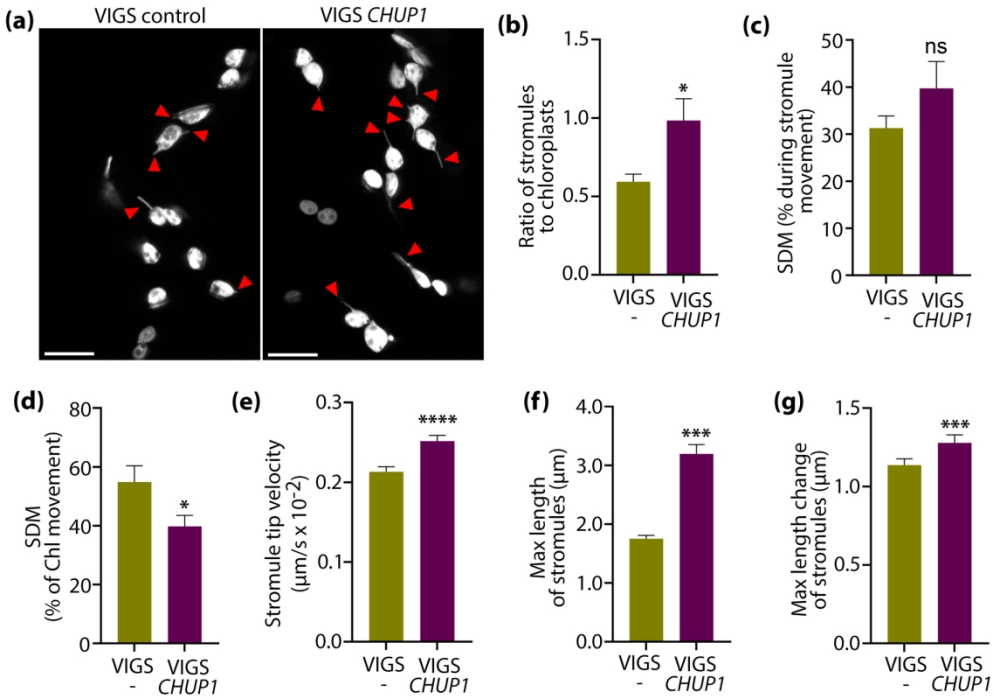

Fig. 4. Silencing *CHUP1* induces stromule amount, velocity, and length.

161x112mm (300 x 300 DPI)

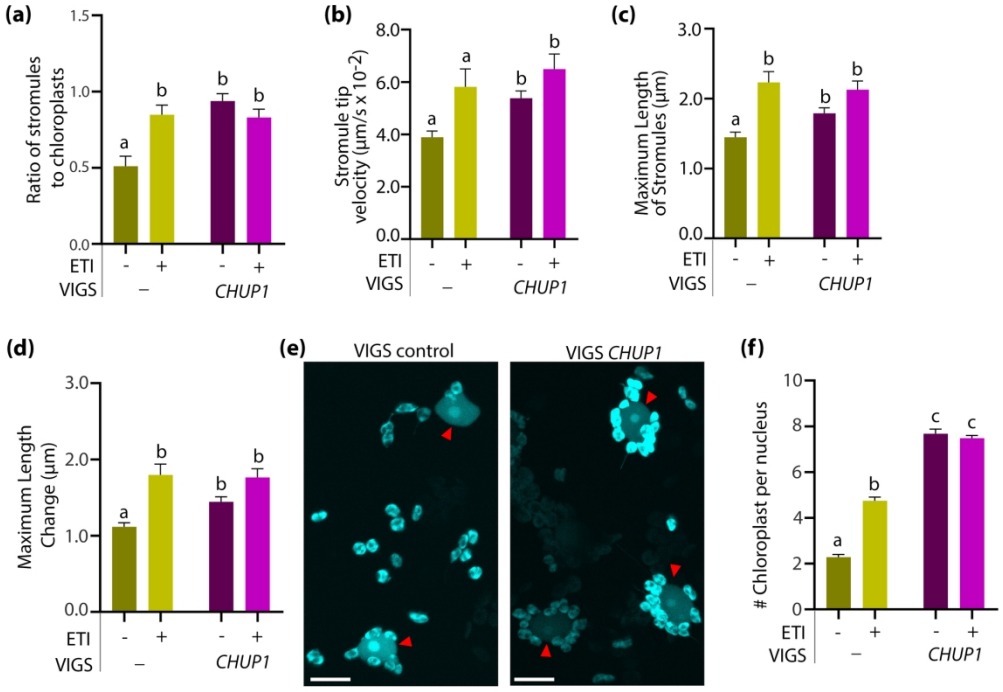

Fig. 5. Silencing *CHUP1* auto-activates chloroplast associated innate immune responses.

179x124mm (300 x 300 DPI)

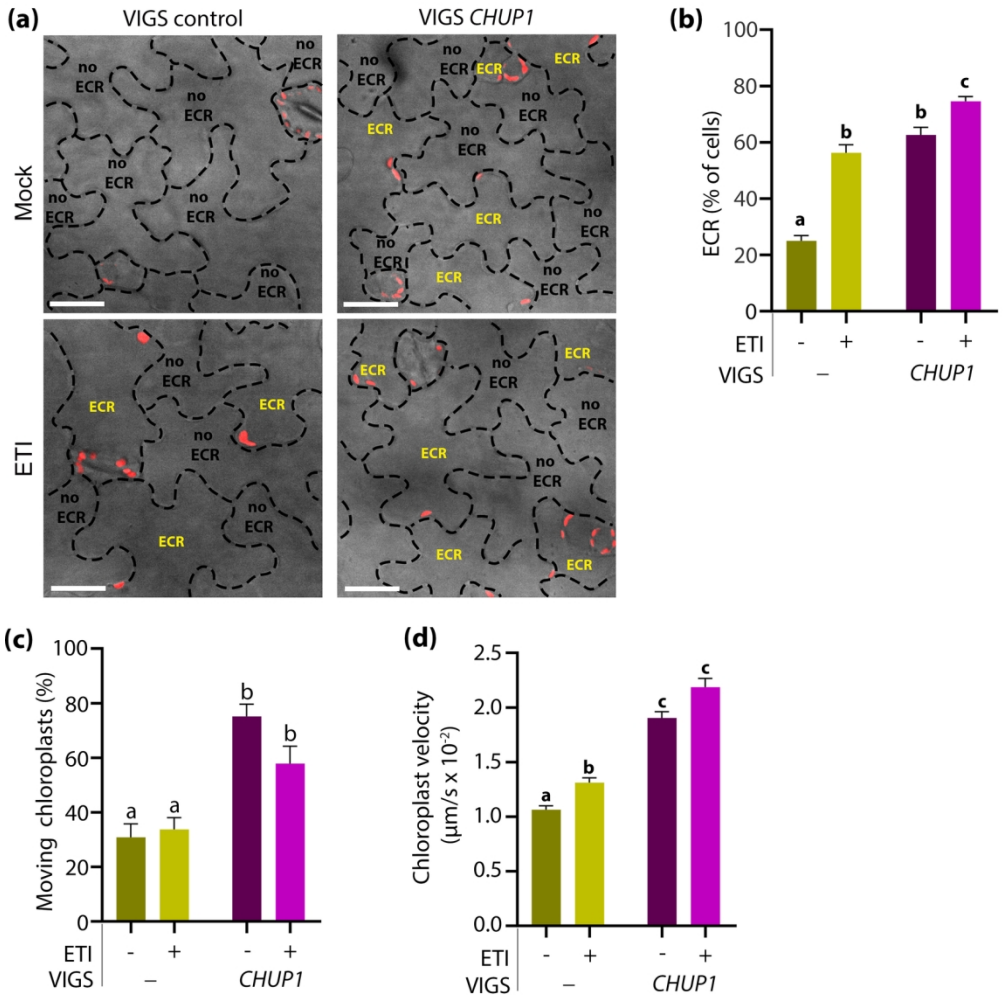

Fig. 6. Epidermal chloroplast response is induced during ETI and by *CHUP1* silencing.

150x150mm (300 x 300 DPI)

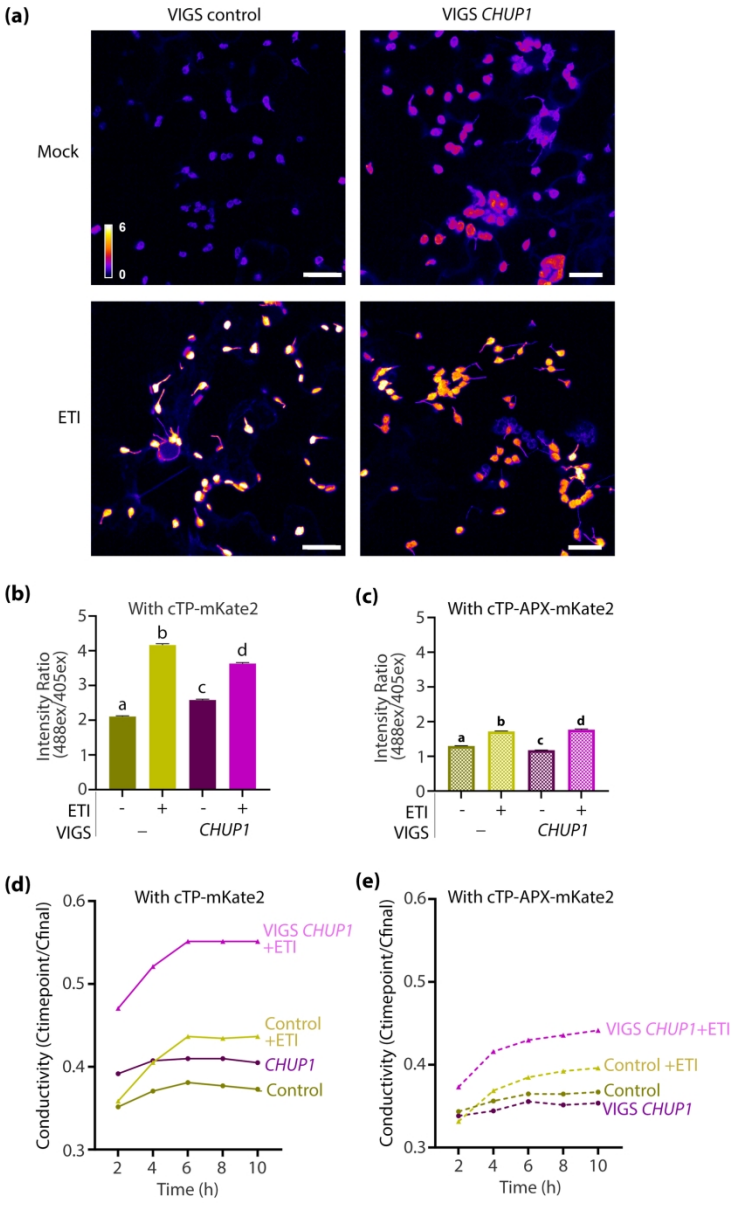

Fig. 7. Hydrogen peroxide is required for enhanced PCD in *CHUP1*-silenced plants.

140x231mm (300 x 300 DPI)

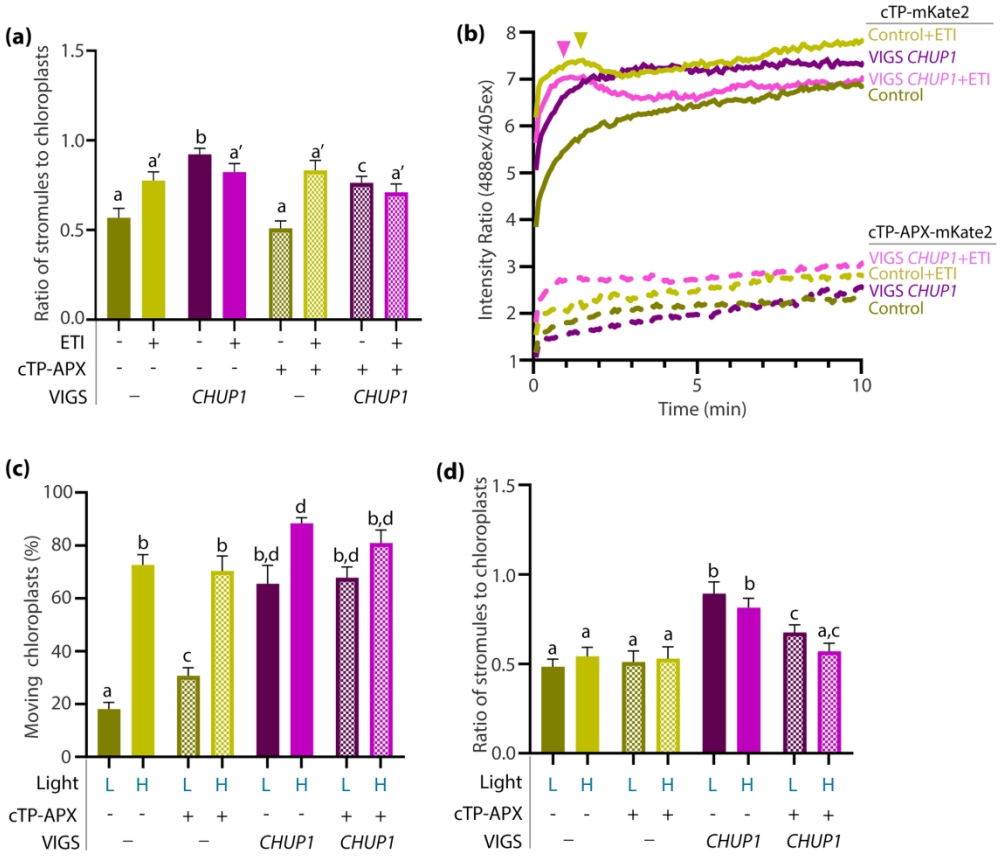

Fig. 8. Hydrogen peroxide is required for stromule induction but not chloroplast movement.

177x152mm (300 x 300 DPI)